SOA

Cl

Cl

Cl

Cl

Cl

Cl

Cl Atom
Generation

Anthropogenic
VOCs

Biogenic
VOCs

ROYAL SOCIETY
OF CHEMISTRY

CRITICAL REVIEW
Lin Du *et al.*
Role of atomic chlorine in atmospheric volatile organic
compound oxidation and secondary organic aerosol
formation: a review

CRITICAL REVIEW

Check for updates

Role of atomic chlorine in atmospheric volatile organic compound oxidation and secondary organic aerosol formation: a review

Yinghong Sun,[a] Li Xu,[a] Jianlong Li,[b] Kun Li, [ID][b] Narcisse Tsona Tchinda [ID][b] and Lin Du [ID] *[abc]

As a highly reactive atmospheric oxidant, chlorine (Cl) atoms significantly contribute to the oxidation of volatile organic compounds (VOCs) and the formation of secondary organic aerosol (SOA) in coastal and industrial environments. To assess the environmental impacts of SOA generated from Cl-initiated oxidation, elucidating its chemical composition, formation mechanisms, and physicochemical properties under varying atmospheric conditions is of paramount importance. This review summarizes recent research advances on atmospheric chlorine chemistry. We first outline the sources and generation mechanisms of Cl atoms, followed by an analysis of the kinetic characteristics, oxidation mechanisms, and SOA formation potential of Cl-initiated VOC oxidation. Compared to hydroxyl (OH) radicals, Cl atoms exhibit faster reaction rates and reaction pathways that preferentially generate low-volatility products, significantly enhancing SOA formation and demonstrating higher SOA yields. Given the complexity of SOA formation and its strong dependence on environmental conditions, we further discuss the responses of gas-phase chemistry as well as SOA mass yields and composition to the $[Cl_2/VOC]_0$ ratios, Cl exposure, NO_x levels, and relative humidity. Finally, we outline key experimental challenges and future research priorities.

Environmental significance

Cl atoms significantly enhance SOA formation through efficient oxidation of VOCs, particularly in coastal and industrial regions. Compared to OH radicals, Cl exhibits higher reactivity and SOA yields. This process is modulated by $[Cl_2/VOC]_0$ ratios, Cl exposure, NO_x levels, and relative humidity, which collectively determine SOA properties by influencing both gas-phase reaction pathways and particle-phase transformations. Current models face limitations in accurately predicting atmospheric pollution due to inadequate mechanistic representation and insufficient parameterization of Cl-initiated SOA formation. This review summarizes the sources and formation mechanisms of Cl, its pivotal role in atmospheric oxidation processes, and environmental dependencies of Cl-SOA formation, thereby providing a foundation for refining parameterization schemes in atmospheric models and enhancing simulation accuracy.

1 Introduction

Fine particulate matter ($PM_{2.5}$) can impact regional air quality by scattering solar radiation and exerting notable impacts on human health and climate change.[1–5] Secondary organic aerosol (SOA) constitutes a significant component of $PM_{2.5}$, accounting for 20–80% on a global scale.[6–9] The formation of SOA involves the oxidation of volatile organic compounds (VOCs) and semi-/intermediate-volatility organic compounds (S/IVOCs), generating low-volatility organic compounds that further undergo

gas-particle partitioning and particle-phase reactions.[10,11] Traditional research has focused on the chemical roles of oxidants such as hydroxyl (OH) radicals,[12–14] ozone (O_3),[15] and nitrate (NO_3) radicals,[16,17] for which relatively comprehensive theoretical frameworks have been established. However, recent studies have identified that the chlorine (Cl) atoms could also be efficient oxidants initiating VOC oxidation and SOA formation (hereafter referred to as "Cl-SOA"),[18–20] especially in coastal or industrial regions, where they contribute to approximately 14.5% of total VOC oxidation and 15% SOA formation.[21–23]

Cl atoms are produced *via* photochemical reactions of chlorine-containing species, which can be formed *via* heterogeneous reactions on sea salt aerosols or directly emitted from coal combustion, biomass burning, water treatment, waste incineration, indoor disinfection, and other industrial processes.[21,24–26] Cl atoms have high reactivity towards VOCs through hydrogen abstraction or addition reactions,[27–31] leading

[a]*School of Environmental Science and Engineering, Shandong University, Qingdao 266237, China. E-mail: lindu@sdu.edu.cn*

[b]*Qingdao Key Laboratory for Prevention and Control of Atmospheric Pollution in Coastal Cities, Environment Research Institute, Shandong University, Qingdao 266237, China*

[c]*State Key Laboratory of Microbial Technology, Shandong University, Qingdao 266237, China*

© 2026 The Author(s). Published by the Royal Society of Chemistry

Environ. Sci.: Atmos., 2026, 6, 7–26 | 7

to 1–2 orders of magnitude higher reaction rate constants than those of OH.[32–36] Therefore, although their concentration (typically 10^2–10^5 molecules per cm^3) is usually one or several orders of magnitude lower than that of OH (typically 10^6 molecules per cm^3),[37–39] they still play a significant role in VOC oxidation.[40–42]

The oxidation of VOCs initiated by Cl atoms and the subsequent formation of SOA involve complex atmospheric processes. Cl atoms can significantly alter the chemistry of other oxidants (e.g., increasing OH and O_3 concentrations by 6–22% and 3–41%, respectively, in polluted continental regions)[43–45] and strengthen the OH–HO_2–RO_2 cycle, thereby elevating the atmospheric oxidation capacity and influencing SOA formation.[46,47] Furthermore, Cl atoms also participate in the direct production processes of SOA formation. Previous studies have shown that the mass yield of Cl-SOA (the ratio of the mass of SOA formed to the mass of precursor consumed) is generally higher than that of SOA driven by OH radicals.[48–50] In addition to increasing SOA concentration, Cl-initiated VOC oxidation can generate multifunctional organochlorides through chlorine substitution, which enhances aerosol toxicity and adversely impacts urban air quality.[21,51,52] However, reported SOA yields and formation mechanisms exhibit substantial variability even for a specific VOC. This variability can be attributed to the differences in the complex environmental conditions including physical parameters (solar intensity, temperature, and relative humidity (RH)),[53,54] inorganic pollutant emissions (NO_x, ammonia, and sulfur dioxide),[41] and oxidant levels ([Cl_2/VOC]$_0$ ratio and Cl exposure (Cl_{exp})).[42] Consequently, Cl-SOA mass yields cannot be represented by fixed values for given precursors. Understanding the dependence of Cl-SOA formation on various environmental conditions is essential for accurately predicting SOA yields and their environmental impacts.
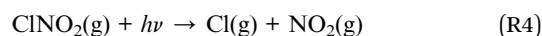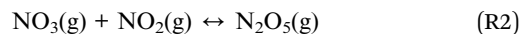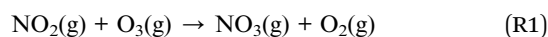
In recent years, numerous studies have been published on Cl atoms as active oxidants participating in the atmospheric oxidation of VOCs and SOA formation. However, existing studies lack a systematic comparison of the reaction rates and SOA yields of different VOCs oxidized by Cl atoms, and the key factors affecting SOA formation have not been fully clarified, which limits the accurate simulation of SOA mass concentration by models. Based on this, this review introduces the sources and generation mechanisms of Cl atoms, systematically summarizes advances in the kinetics and mechanisms of Cl-initiated VOC oxidation, and further discusses the yield and influencing factors of SOA. By integrating the latest experimental research, this paper aims to provide a theoretical foundation for establishing more accurate parameterization schemes for chlorine chemistry, thereby improving model quantification of Cl-SOA generation.

2 Sources and generation mechanisms of Cl atoms

Cl atoms are primarily generated through the photolysis of reactive chlorine species during daytime, with precursors including nitryl chloride ($ClNO_2$), Cl_2, hypochlorous acid

(HOCl), hydrochloric acid (HCl), and chloramines. These reactive chlorine species originate from diverse sources. HCl can be released from natural sources such as volcanic eruptions,[45] while anthropogenic activities including coal combustion municipal solid waste incineration, industrial processes, biomass burning, and disinfectant usage can emit HCl, Cl_2, chloramines, and HOCl.[24–26] For instance, in downtown Toronto, the mean daily peak mixing ratios of monochloramine and dichloramine during summer approached 500 and 250 ppt, respectively. The photolysis of chloramines can be a substantial contributor to Cl atom production, particularly in urban environments.[55] Similarly, HOCl present in bleach solutions can volatilize into the gas phase after indoor use, reaching concentrations of up to 200 ppb during certain disinfection activities.[56] Recent studies have observed high concentrations of Cl_2 and $ClNO_2$ in coastal areas, where these species are predominantly formed through secondary chemical processes involving heterogeneous reactions between sea salt aerosols and gaseous species, as well as photochemical reactions.[23,57] Notably, anthropogenic activities can also produce substantial particulate chlorides, which can undergo secondary chemical processes to generate precursors of reactive chlorine species.[24,25] This mechanism may contribute to elevated concentrations of species such as $ClNO_2$ and Cl_2 observed in inland regions. The following sections will elaborate on these secondary formation mechanisms for reactive chlorine species and the formation process of Cl atoms.
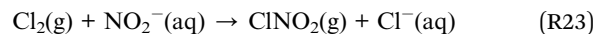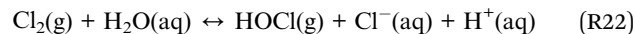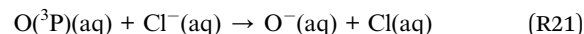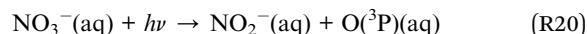
$ClNO_2$ is a major source of Cl atoms in coastal and inland regions during morning hours. Its formation is predominantly achieved through a chain of nocturnal atmospheric chemical reactions: first, NO_x reacts with O_3 to form NO_3 radicals (R1), which then combine with NO_2 to produce dinitrogen pentoxide (N_2O_5) (R2). N_2O_5 subsequently undergoes heterogeneous reactions on chloride-containing aerosol (Cl^-) surfaces to generate $ClNO_2$ (R3).[58–62] Field observations indicate that under specific conditions, its concentration can reach parts per billion (ppb) levels.[63] The $ClNO_2$ accumulated overnight undergoes rapid photolysis after sunrise, which not only directly releases highly reactive Cl atoms to enhance atmospheric oxidation capacity, but also sustains the NO_x cycle by regenerating NO_2 (R4).

$$NO_2(g) + O_3(g) \rightarrow NO_3(g) + O_2(g) \tag{R1}$$

$$NO_3(g) + NO_2(g) \leftrightarrow N_2O_5(g) \tag{R2}$$

$$N_2O_5(g) + Cl^-(aq) \rightarrow ClNO_2(g) + NO_3^-(aq) \tag{R3}$$

$$ClNO_2(g) + h\nu \rightarrow Cl(g) + NO_2(g) \tag{R4}$$

In addition to $ClNO_2$, Cl_2 is another important precursor of Cl atoms in the lower troposphere.[19] Observations of nocturnal peaks or daytime increases in Cl_2 concentrations in coastal and continental regions suggest multiple generation pathways.[23,64,65] First, Cl_2 can be produced via heterogeneous reactions of $ClNO_2$, HOCl, chlorine nitrate ($ClONO_2$), and OH with chloride in aerosols, a process known as autocatalytic chlorine activation

(R5)–(R8).[57,66–69] Xia *et al.* hypothesized that the Cl_2 observed in suburban areas of eastern China was more likely a co-product with $ClNO_2$ from N_2O_5 uptake on acidic aerosols that contain chloride than being produced by $ClNO_2$ uptake as previously suggested.[70] In Arctic regions, laboratory experiments, model simulations, and field observations showed that O_3 photolysis on liquid sea salt particles, saline snow, or ice surfaces is an important way for Cl_2 formation (R9).[71–73] Beyond these processes, Cl_2 is also proposed to be efficiently generated through the photolysis of aerosols containing Fe(III) and chloride, as well as particulate nitrate. For example, Chen *et al.* proposed an aerosol iron photochemistry-driven Cl_2 formation mechanism (R10)–(R16), accounting for over 90% of Cl_2 production in northern China.[74] van Herpen *et al.* further proposed that aerosol-phase iron photochemistry serves as the dominant source of Cl_2 and Cl atoms over the North Atlantic, where iron-rich mineral dust aerosols from the Sahara mix with sea spray aerosols.[75] Recently, Peng *et al.* identified aerosol nitrate photolysis as the dominant daytime source of Cl_2 in Hong Kong.[18] OH radicals from nitrate photolysis and subsequent oxidation of chloride in solution can further oxidize Cl^- to produce Cl_2 ((R12)–(R16), (R18) and (R19)). Nitrate photolysis can also produce nitrite (NO_2^-) and ground-state oxygen atoms $O(^3P)$, where the oxidation of Cl^- by $O(^3P)$ provides an additional pathway for Cl_2 formation ((R12)–(R16), (R20) and (R21)).[76,77] Notably, in the presence of $Cl^-(aq)$, the Cl_2 generated from nitrate photolysis can further react to form HOCl (R22).[78] Both Cl_2 and HOCl can then react with NO_2^-, leading to the production of $ClNO_2$ ((R23) and (R24)).[79,80] This mechanism should be incorporated into chemical models to better understand heterogeneous oxidation chemistry and halogen cycling.

$$ClNO_2(g) + H^+(aq) + Cl^-(aq) \rightarrow Cl_2(g) + HNO_2(g) \quad (R5)$$

$$HOCl(g) + H^+(aq) + Cl^-(aq) \rightarrow Cl_2(g) + H_2O(aq) \quad (R6)$$

$$ClONO_2(g) + H_2O(g) + Cl^-(aq) \rightarrow Cl_2(g) + HNO_3(g) \quad (R7)$$

$$OH(g) + Cl^-(aq) \rightarrow 0.5Cl_2(g) + OH^-(aq) \quad (R8)$$

$$O_3(g) + 2Cl^-(aq) \rightarrow Cl_2(g) + 2OH^-(aq) + O_2(g) \quad (R9)$$

$$FeCl^{2+}(aq) + h\nu \rightarrow Fe^{2+}(aq) + Cl(aq) \quad (R10)$$

$$FeCl_2^+(aq) + h\nu \rightarrow FeCl^+(aq) + Cl(aq) \quad (R11)$$

$$Cl(aq) + Cl^-(aq) \leftrightarrow Cl_2^-(aq) \quad (R12)$$

$$Cl(aq) + Cl_2^-(aq) \leftrightarrow Cl^-(aq) + Cl_2(aq) \quad (R13)$$

$$Cl_2^-(aq) + Cl_2^-(aq) \rightarrow Cl^-(aq) + Cl_3^-(aq) \quad (R14)$$

$$Cl_3^-(aq) \leftrightarrow Cl_2(aq) + Cl^-(aq) \quad (R15)$$

$$Cl_2(aq) \leftrightarrow Cl_2(g) \quad (R16)$$

$$Cl_2(g) + h\nu \rightarrow 2Cl(g) \quad (R17)$$

$$NO_3^-(aq) + H^+(aq) + h\nu \rightarrow NO_2(aq) + OH(aq) \quad (R18)$$

$$OH(aq) + Cl^-(aq) + H^+(aq) \rightarrow Cl(aq) + H_2O(aq) \quad (R19)$$

$$NO_3^-(aq) + h\nu \rightarrow NO_2^-(aq) + O(^3P)(aq) \quad (R20)$$

$$O(^3P)(aq) + Cl^-(aq) \rightarrow O^-(aq) + Cl(aq) \quad (R21)$$

$$Cl_2(g) + H_2O(aq) \leftrightarrow HOCl(g) + Cl^-(aq) + H^+(aq) \quad (R22)$$

$$Cl_2(g) + NO_2^-(aq) \rightarrow ClNO_2(g) + Cl^-(aq) \quad (R23)$$

$$HOCl(g) + NO_2^-(aq) \rightarrow ClNO_2(g) + OH^-(aq) \quad (R24)$$

HOCl represents a significant chlorine precursor species, with elevated concentrations observed during autumn 2022 in coastal cities of southeastern China, where the average daytime peak level reached 181 ppt.[81] Previous studies have identified Cl_2, O_3, nitrate, and iron as critical factors in HOCl formation. In the presence of O_3, photolysis of Cl_2, nitrate photolysis, and aerosol-phase iron photochemistry lead to daytime HOCl production through reactions of ClO and hydroperoxyl radicals (HO_2) ((R25) and (R26)).[68,81,82] Furthermore, ClO can react with NO_2 to form $ClONO_2$, whose hydrolysis also generates HOCl ((R27) and (R28)).[83] The photolysis of HOCl produces OH radicals and Cl atoms (R29), which can oxidize VOCs to promote RO_x radical and O_3 formation, significantly enhancing the atmospheric oxidation capacity. However, under real atmospheric conditions, the rates of HOCl generation *via* nitrate photolysis and aerosol iron photochemistry are influenced by multiple factors—such as aerosol acidity, particulate chloride content, nitrate concentration, iron speciation, and aerosol surface area—many of which remain unquantified. Therefore, future laboratory studies are needed to refine our understanding of these mechanisms.

$$Cl(g) + O_3(g) \rightarrow ClO(g) + O_2(g) \quad (R25)$$

$$ClO(g) + HO_2(g) \rightarrow HOCl(g) + O_2(g) \quad (R26)$$

$$ClO(g) + NO_2(g) + M \rightarrow ClONO_2(g) + M \quad (R27)$$

$$ClONO_2(g) + H_2O(aq) \rightarrow HOCl(g) + HNO_3(aq) \quad (R28)$$

$$HOCl(g) + h\nu \rightarrow Cl(g) + OH(g) \quad (R29)$$

$$HCl(g) + OH(g) \rightarrow Cl(g) + H_2O(g) \quad (R30)$$
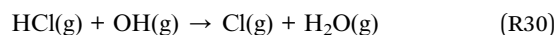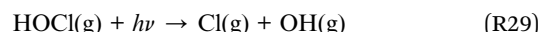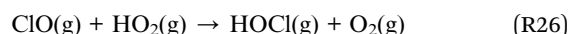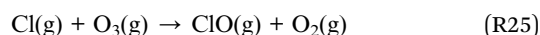
As discussed above, the photolysis of $ClNO_2$, Cl_2, and HOCl can all generate Cl atoms ((R4), (R17), and (R29)). Cl atoms can be regenerated through heterogeneous cycling on chloride-containing aerosols or *via* volatilization and subsequent oxidation of HCl (R30).[84] Since current measurement techniques cannot precisely determine atmospheric Cl concentrations, they are typically estimated based on precursor photolysis rates. The global average atmospheric Cl concentration is estimated to be approximately 10^3 molecules per cm^3, while in coastal regions it can reach 10^4–10^5 molecules per cm^3.[85,86] Recent studies have shown that even in some inland areas, such as the North China Plain, peak Cl concentrations can reach 10^5 molecules per cm^3.[19,65] These findings robustly demonstrate

© 2026 The Author(s). Published by the Royal Society of Chemistry

Environ. Sci.: Atmos., 2026, **6**, 7–26 | **9**

that the potential contribution of Cl atoms to atmospheric oxidation capacity in inland urban areas cannot be ignored.[46]

3 Atmospheric oxidation of VOCs by Cl atoms: kinetics and mechanism

3.1 Rate constants for reactions of Cl atoms with organic compounds

Fig. 1 summarizes the gas-phase reaction rate constants (k_{Cl}) of Cl atoms with 716 organic compounds, which are the combined rate constant through addition and abstraction channels.[87,88] The compounds are divided into 13 groups, including alkanes, alkenes, alkynes, aromatic compounds, alcohols, ethers, aldehydes, ketones, esters, carboxylic acids, nitrogen compounds, sulfur compounds, and halogenated compounds (See Table S1 in the SI). By comparing the average reaction rate constants of each group, it is evident that their reactivity varies significantly. Specifically, alkenes exhibit higher average reaction rate constants (4.36×10^{-10} cm^3 per molecule per s) than alkanes (3.24×10^{-10} cm^3 per molecule per s) due to the presence of carbon–carbon double bonds, which provide favorable addition sites for Cl atoms.[89] Although alkynes contain unsaturated triple bonds, their reactivity with Cl atoms (5×10^{-11} cm^3 per molecule per s) is lower than those of alkenes and alkanes because the electron density in triple-bonded carbons is more concentrated, resulting in greater steric hindrance.[33] Aromatic compounds generally exhibit lower reactivity toward Cl atoms compared to alkanes and alkenes. This difference stems primarily from the resonance stabilization provided by the conjugated π-electron system of the aromatic ring, which substantially increases the activation energy required for direct attack on the aromatic ring. As a result, Cl atoms do not readily undergo direct hydrogen abstraction or addition reactions with aromatic systems as they do with alkanes or alkenes. In most

cases, particularly when the aromatic ring carries substituents such as alkyl groups, Cl atoms preferentially abstract hydrogen atoms from these substituents, while the presence of carbon–carbon double bonds within the substituent may promote addition reactions.[28,33] The average reaction rate constants show relatively small differences among oxygenated organic compounds (including alcohols, ethers, aldehydes, ketones, and esters). A study suggested that the activating effect of oxygen atoms may cause certain ethers to exhibit higher reactivity than their corresponding alkanes.[90] However, unsaturated alcohols, esters, and aldehydes generally have lower rate constants for their reactions with Cl atoms compared to those of corresponding alkenes. This is attributed to the negative inductive effects of hydroxyl (–OH), ester (–COOR), and aldehyde (–CHO) groups, which reduce the reactivity of double bonds toward electrophilic addition by Cl atoms.[91,92] Additionally, carboxylic acids display particularly low reactivity due to the strong polarity and significant steric hindrance of their carboxyl groups. For nitrogen-, sulfur-, and halogen-containing compounds, the presence of heteroatoms alters molecular electronic structures and chemical properties, resulting in diverse reactivity patterns.

Within the same class of compounds, the reaction rate constants are influenced by the molecular structure, including the carbon chain length, the degree of branching, and the type, number, and position of substituents. For alkanes, the reactivity ratio of primary, secondary, and tertiary C–H bonds with Cl atoms is $1.0 : 3.8 : 5.5$, and the reaction rate constant increases with carbon chain length, while the branching position has a minimal impact.[93–95] In small alkenes (e.g., propene and 1-butene), the hydrogen abstraction is negligible, but as the carbon chain length increases (by –CH$_2$– insertion), the hydrogen abstraction becomes more significant, and the reaction rate constant increases. The reactivity of alkenes strongly depends on the position of the double bond, with terminal alkenes being more reactive than internal alkenes, and conjugated dienes exhibiting even higher reactivity.[33] This is because Cl atom addition to terminal carbons forms secondary radicals centered on the second carbon, which are more stable than primary radicals formed by addition to internal carbons.[89] The reaction rate constant of toluene is 2.5×10^5 times higher than that of benzene, indicating that Cl atoms primarily react with toluene via hydrogen abstraction from the methyl group. Similarly, the rate constants of toluene, xylene, and trimethylbenzene increase linearly with the number of methyl substituents (each methyl group contributes $(6–8) \times 10^{-11}$ cm^3 per molecule per s), while the substituent position (e.g., in xylene) has little effect. Likewise, alkyl-naphthalenes exhibit rate constants up to 100 times higher than that of naphthalene, increasing with the number of available alkyl hydrogens.[28] The same trend is observed for oxygenated organic compounds, with studies showing that the reaction rate constants of alcohols,[92] ethers,[90] aldehydes,[29] ketones,[96] esters,[97] and furans[98] increase with carbon chain length. Notably, inserting a –CH$_2$– group between the oxygen atom and the double bond in unsaturated esters reduces the reaction rate constant, as this disrupts the conjugation between the lone pair electrons on the
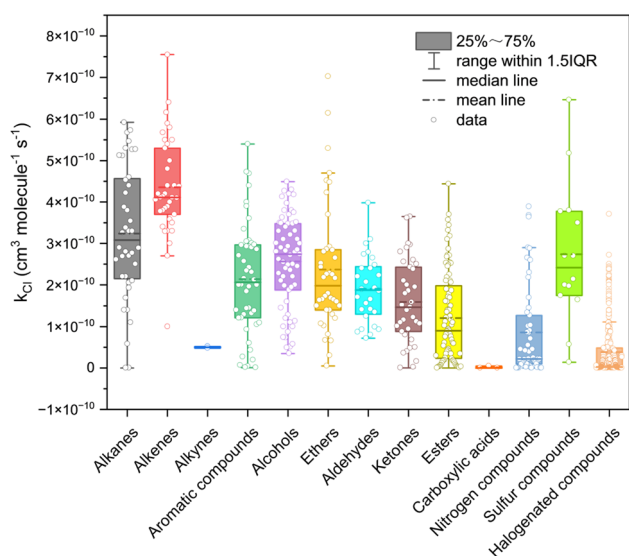

Fig. 1 Rate constants for reactions of Cl atoms with organic compounds. Data from the database for the kinetics of the gas-phase atmospheric reactions of organic compounds.[87,88]

ester oxygen and the π-electron system of the double bond.[97] For unsaturated aldehydes with a central double bond, branching with electron-donating methyl groups accelerates the reaction, but the position of the methyl group has little effect on Cl atom reactivity.[29] Furthermore, a comparison of the reaction rates between 2-butanone and 2,3-butanedione (or acetone and 2,3-butanedione) reveals that introducing additional carbonyl groups significantly diminishes the reactivity toward Cl atoms.[96] Thus, the rate constants for reactions of Cl atoms with organic compounds within the same class exhibit discrete distributions.

Although significant progress has been made in the kinetics of Cl atoms gas-phase reactions, the number of compounds covered by experimental data remains limited compared to those with OH radicals. Moreover, the influence of environmental conditions (*e.g.*, temperature and pressure) on reaction kinetics has not yet been fully elucidated. Future research should develop more precise experimental techniques, establish comprehensive structure–activity relationships, and enhance simulations of reaction kinetics under real-world environmental conditions.

3.2 Comparison of rate constants for reactions of Cl atoms and OH radicals

The ratios of rate constants for reactions of Cl atoms and OH radicals with selected typical atmospheric VOCs are summarized in Fig. 2. The results show that Cl atoms exhibit reaction rate constants 1–2 orders of magnitude higher than that of OH radicals for most organic compounds. Taking alkanes as an example, Cl atoms initiate reactions *via* hydrogen abstraction, forming HCl and RO_2. According to the structure–activity relationship, Cl atoms abstract terminal hydrogens more frequently than OH radicals, leading to different product distributions.[99] Consequently, the reaction rate constants of Cl atoms with alkanes are an order of magnitude higher than those of OH radicals. Additionally, based on gas collision theory, the reaction rate constants of Cl atoms approach the gas-kinetic limit, enabling high reactivity across diverse VOCs.[91,100] Considering the concentrations of both oxidants and their reaction rate constants with atmospheric organic compounds, Cl atoms may contribute approximately 10–100% to organic compound transformation compared to OH radicals. With recent discoveries of inland chlorine sources, the total atmospheric chlorine

production has risen substantially, breaking geographical limitations in atmospheric organic compound transformation.[44] Notably, in some regional contexts, Cl atoms contribute more to alkane transformation than OH radicals.[59] These findings suggest that the traditional OH-dominated atmospheric oxidation paradigm requires revision, particularly in regions with enhanced chlorine sources, where chlorine chemistry must be fully integrated into assessments of atmospheric oxidation and secondary pollutant formation.

3.3 Reaction mechanism

The primary VOC species emitted into the atmosphere consist of alkanes, alkenes, aromatic hydrocarbons, and oxygenated volatile organic compounds (OVOCs).[101,102]

These compounds are efficiently oxidized by atmospheric Cl atoms to form RO_2 radicals. RO_2 can react with HO_2, RO_2, or NO: (1) reactions between RO_2 and HO_2 typically produce hydroperoxides; (2) RO_2 self- or cross-reactions form carbonyls, alcohols, or alkoxy radicals (RO); (3) the reaction of RO_2 with NO usually leads to organic nitrates and RO.[11,103,104] This section focuses on reaction mechanisms in the absence of NO_x, while the reaction pathways of RO_2 with NO will be discussed in Section 4.2.2. Beyond these pathways, RO_2 can also undergo isomerization/autoxidation, generating multifunctional oxygenated compounds such as highly oxidized organic molecules (HOMs).[48,105] The aforementioned pathways are present in both OH- and Cl-initiated oxidation processes. However, in Cl-initiated oxidation, RO_2 radicals can additionally react with Cl atoms to form RO and ClO. The resulting ClO can further react with RO_2, potentially leading to the formation of ROCl.[106,107] These products can undergo further oxidation and condensation, significantly contributing to the formation of SOA. Although the oxidation mechanisms described above provide a general framework, specific reaction pathways and dominant products exhibit substantial differences across various classes of compounds.

For alkanes, taking linear alkanes as an example, their reaction with Cl atoms proceeds *via* hydrogen abstraction, involving two types of reaction sites: internal hydrogen atoms (methylene H) and terminal hydrogen atoms (methyl H), as illustrated in Fig. 3a.[94] The alkyl radicals generated through hydrogen abstraction rapidly react with O_2 to form RO_2. These
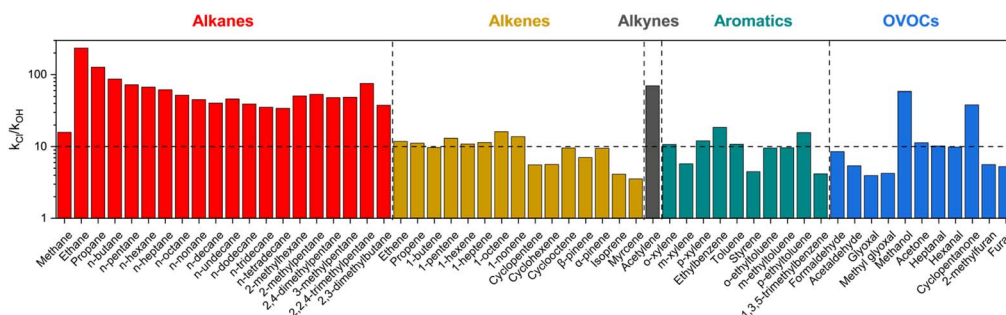

Fig. 2 Comparison of rate constants for reactions of Cl atoms and OH radicals with typical VOCs. The black horizontal dashed line represents a k_{Cl}/k_{OH} ratio of 10.
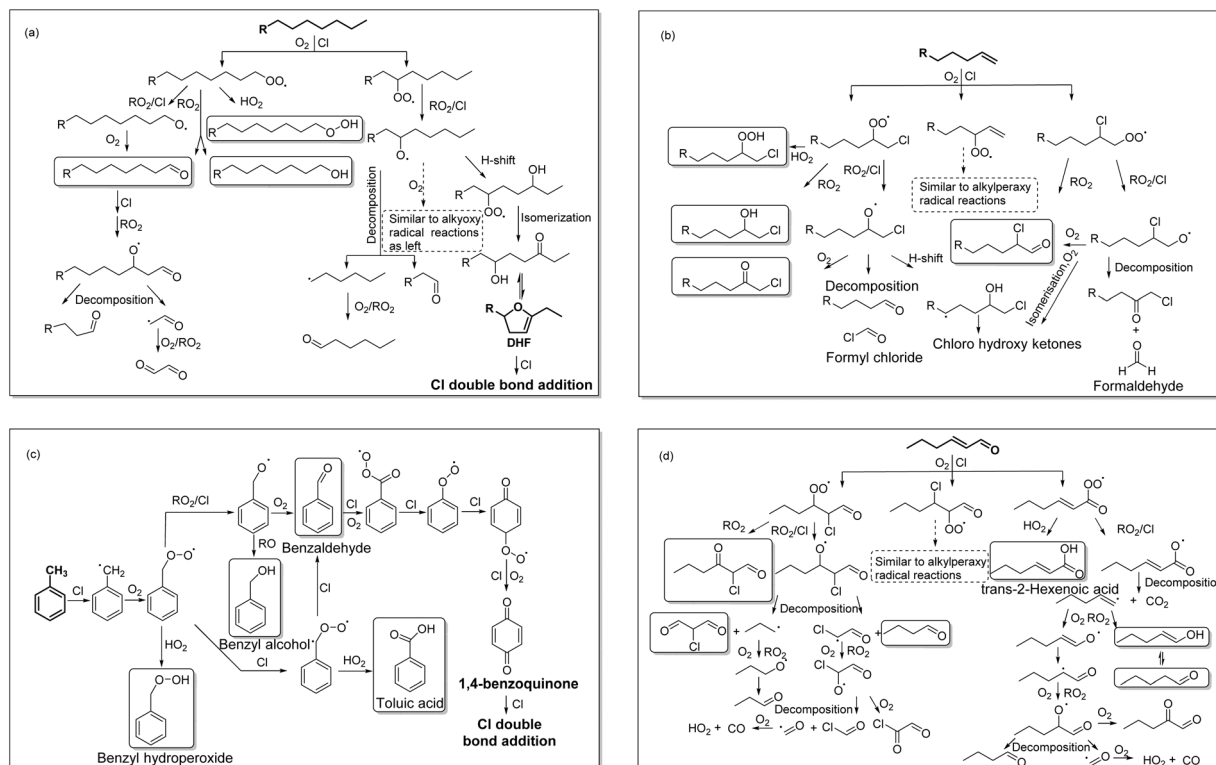
© 2026 The Author(s). Published by the Royal Society of Chemistry

Environ. Sci.: Atmos., 2026, **6**, 7–26 | 11

Fig. 3 Mechanism of Cl-initiated oxidation of VOCs in the absence of NO$_x$: (a) alkane; (b) alkene; (c) aromatic hydrocarbon; (d) OVOC. Subsequent products formed from the initial RO$_2$ radicals are indicated in boxes.

RO$_2$ radicals subsequently undergo conversion predominantly to RO radicals, which then proceed through three primary pathways for further oxidation: (1) reaction with O$_2$ to form carbonyl compounds and HO$_2$, where the resulting carbonyl compounds can be further oxidized by Cl atoms; (2) direct decomposition into small oxygenated molecules; (3) intramolecular hydrogen transfer to produce hydroxycarbonyl compounds. Notably, in this third pathway, the resulting 1,4-hydroxycarbonyl compounds undergo acid-catalyzed isomerization and dehydration, leading to the heterogeneous production of dihydrofuran (DHF).[108–110] Subsequent Cl atom addition to the DHF double bond may serve as a source of organic chlorides.[111]

For alkenes, a general reaction scheme involving RO$_2$ and RO radicals is proposed (Fig. 3b). The reaction between Cl atoms and alkenes primarily proceeds via Cl addition to the double bond, with hydrogen abstraction playing a minor role. For example, the branching ratio for methyl H abstraction in Cl-isoprene ranges from 0.13 to 0.17. The NASA JPL data evaluation recommends a branching fraction of 0.15 at 298 K to form HCl, which is the mean value observed in the studies of Cl-isoprene.[112–115] The initial reaction generates chloroalkyl radicals and alkenyl radicals (centered at different carbon atoms), which rapidly react with atmospheric O$_2$ to form RO$_2$. These RO$_2$ radicals subsequently undergo conversion predominantly to RO radicals.[116] Similar to alkanes, the resulting RO radicals can react with O$_2$ or decompose to form carbonyl compounds.[52] Additionally, these RO radicals may undergo isomerization

pathways, such as hydrogen transfer, leading to the formation of compounds like chlorohydroxy ketones. Experimental studies have detected gaseous products including chlorinated ketones, chlorinated alcohols, enones, and enols, among which low-volatility alcohols and ketones can undergo heterogeneous reactions on aerosol surfaces or directly condense into the particle phase to form SOA.[117]

The reaction with aromatic hydrocarbons is also an important atmospheric sink for Cl atoms. Unlike OH radicals, the mechanisms of reactions of Cl atoms with aromatic hydrocarbons exhibit distinct differences: OH typically initiates oxidation preferably via addition to the aromatic ring, whereas Cl tends to directly abstract hydrogen atoms from alkyl side chains, thereby triggering subsequent free-radical chain reactions (Fig. 3c).[49] For instance, Cl-initiated oxidation of toluene primarily proceeds via hydrogen abstraction from the methyl group to form a benzyl radical, which subsequently reacts with O$_2$ to yield a benzyl peroxy radical.[28] The subsequent reactions of this radical follow three main pathways: (1) reaction with a HO$_2$ radical to form benzyl hydroperoxide; (2) reaction with Cl atoms via hydrogen abstraction to generate a benzyl Criegee biradical, which can further react with water to produce benzoic acid or with Cl atoms to form benzaldehyde; (3) direct conversion to the corresponding alkoxy radical via reaction with Cl atoms, followed by reaction with O$_2$ to form benzaldehyde. The benzyl peroxy radical may also undergo self-reaction to produce benzyl alcohol and benzyl dimers.[42] Experimental studies have confirmed that benzaldehyde, benzyl alcohol, and benzyl

12 | *Environ. Sci.: Atmos.*, 2026, **6**, 7–26

© 2026 The Author(s). Published by the Royal Society of Chemistry

hydroperoxide are the three major gaseous products of toluene oxidation by Cl atoms.[28,118,119] Notably, the abstraction of the aldehyde H from benzaldehyde forms a benzoyl radical, which can be further oxidized to generate 1,4-benzoquinone and other quinone-like compounds. The two endocyclic double bonds of quinone-like compounds may then be further oxidized by Cl atoms.

OVOCs extensively participate in key atmospheric processes and play a central role in chemical processes that determine the oxidizing capacity of the atmosphere. Current research predominantly focuses on unsaturated OVOCs.[120–123] Fig. 3d illustrates the mechanism of reactions of Cl atoms with unsaturated aldehydes, using *trans*-2-hexenal as an example. Unsaturated aldehydes containing carbonyl groups and carbon–carbon double bonds typically undergo two types of reactions when interacting with Cl atoms in the atmosphere: Cl addition and H-abstraction. Based on previous experimental and theoretical studies of Cl reactions with unsaturated hydrocarbons, allylic H-abstraction is a minor pathway and thus is not considered in this work.[124] The addition pathway proceeds as described above for alkenes; the decomposition of the chloroalkoxy radicals leads to the formation of aldehydes and chlorinated compounds, such as formyl chloride. CO is also formed as a by-product of formyl chloride. In the H-abstraction pathway, the removal of the formyl H generates acyl radicals and HCl. Subsequently, the acyl radicals rapidly react with O_2 to form acyl peroxy radicals, the key intermediate that undergoes two competitive pathways: (1) reaction with HO_2 to produce 2-hexenoic acid and O_3; (2) reaction with RO_2 or Cl atoms to generate RO radicals, which then decompose to form alkenyl radicals and CO_2. The alkenyl radicals, converted into alkenyl peroxy radicals in the presence of O_2, further react with RO_2 to produce aldehydes.[125]

Although current understanding of atmospheric degradation processes for most Cl-VOCs has been established to some extent, the description of chlorine chemistry in the Master Chemical Mechanism (MCM) remains incomplete. The MCM is one of the most widely deployed chemical mechanisms, which explicitly describes the degradation of 143 primarily emitted VOCs initiated by OH, O_3, and NO_3. However, it only considers Cl reactions with alkanes (22 species), and assumes the formation of the same peroxy radicals as in OH oxidation, with no subsequent Cl-specific reactions. A previous study has supplemented the mechanisms and kinetic data (*e.g.*, rate constants and branching ratios) for the initial oxidation of VOCs (65 species) initiated by Cl atoms, but subsequent reaction mechanisms involving the further oxidation of intermediate products are still lacking.[126] Table S2 summarizes the key missing pathways in Cl-initiated oxidation within the current chemical mechanism. As outlined in the table, although current experiments have preliminarily deduced partial reaction mechanisms based on characteristic oxidation products, the lack of key chemical pathways and kinetic parameters severely restricts the construction of chlorine chemistry mechanisms. Therefore, further in-depth investigation into the detailed oxidation mechanisms of Cl atoms with various VOCs (particularly alkenes and aromatic hydrocarbons) is essential for

improving the accuracy of atmospheric chemical model simulations.

4 SOA formation from Cl-initiated oxidation

As atmospheric oxidation reactions proceed, the increasing functionalization of oxidation products leads to a decrease in their vapor pressure. These products with low volatility readily contribute to SOA formation through nucleation, condensation, and particle-phase reactions.[127,128] This section synthesizes laboratory studies on Cl-SOA, addressing both SOA yield and the factors influencing SOA formation.

4.1 SOA yield

SOA yield is an important parameter for model simulation and laboratory research. The data presented in Fig. 4 include Cl-SOA yields from different precursors under various atmospheric conditions, primarily involving VOCs such as alkanes, alkenes, and aromatic hydrocarbons. For comparison, we also compiled the yield ranges of OH-initiated SOA (OH-SOA) under similar conditions (Table S3).

Fig. 4 shows that Cl- and OH-SOA yields generally follow similar trends across different precursors. However, for a given precursor, Cl-SOA yields are often higher than OH-SOA yields. The key reason lies in the preference for initial H-abstraction sites and the relative importance of H-abstraction pathways, which fundamentally alter subsequent reaction pathways. In systems where H-abstraction is the dominant reaction pathway (*e.g.*, alkanes), Cl tends to abstract primary H-atoms at the chain ends, whereas OH primarily abstracts secondary H-atoms along the chain.[129] Radicals generated from primary carbon H-abstraction are more likely to undergo functionalization, forming low-volatility oxygenated products rather than carbon-chain fragmentation, thereby preserving larger carbon skeletons and producing low-volatility species. In contrast, OH preferentially attacks secondary/tertiary carbon sites, leading to
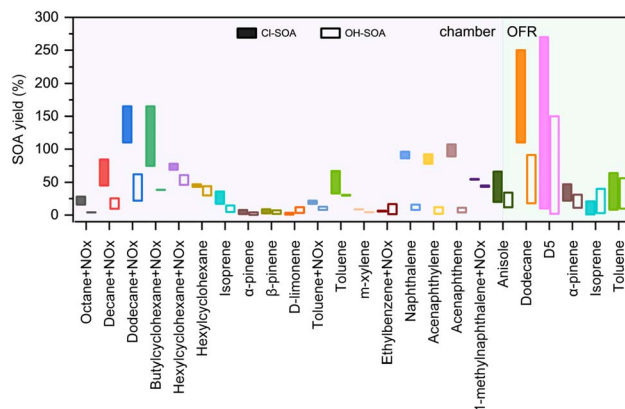

Fig. 4 A comparison of SOA yields from VOC oxidation initiated by Cl atoms *versus* OH radicals was conducted using different reactor systems, specifically chambers[40,48–50,53,111,116,129–138] and oxidation flow reactors (OFRs).[107,139,140] D_5 stands for decamethylcyclopentasiloxane.

subsequent β-scission reactions that generate smaller, volatile fragments.[48,103] Additionally, due to its lower reactivity towards oxygenated functional groups such as aldehydes, Cl allows oxidation intermediates to retain polar groups that participate in condensation, while OH rapidly degrades these functional groups, causing molecular fragmentation.[111,130] These characteristics collectively result in higher SOA yields from Cl oxidation compared to OH oxidation under the same conditions.

For monoaromatic and polycyclic aromatic hydrocarbons, Cl enhances the relative importance of H-abstraction pathways in multigenerational oxidation compared to OH-dominated systems. Cl-initiated H-abstraction can occur both in the reaction of the parent VOC and in the reaction of oxidation products (*e.g.*, phenolic –OH groups).[50,53,135] Unlike OH, which primarily adds to aromatic rings and forms ring-opening products, Cl-driven aromatic oxidation mainly proceeds *via* H-abstraction, generating ring-retaining products that more readily condense into the particle phase.[40,49,141] H-abstraction from phenolic groups by Cl directly forms phenoxy radicals, which are critical for accurately modeling nitrophenol formation and radical and ozone cycling in ambient environments.[53,142] Given the increasing concentrations of reactive chlorine species and the fact that Cl demonstrates higher reaction rates and SOA yields than OH for most VOCs, the role of chlorine chemistry in the atmosphere needs to be reconsidered.

As discussed above, for a given precursor, the SOA yields initiated by Cl atoms are generally higher than that by OH radicals. However, the contribution of Cl-SOA has not been adequately accounted for in current models. Recently, Liu *et al.* developed a Cl-SOA simulation module in a global chemical transport model by integrating parameterized SOA yields and updated anthropogenic continental chlorine emissions. Their results demonstrate that incorporating chlorine chemistry can significantly enhance SOA formation in polluted urban environments and help reduce biases in current model simulations.[21] To bridge laboratory Cl-SOA results with modeling applications, we have developed a parameterization scheme for Cl-SOA yields (Table S4). The scheme provides median yields and their uncertainty ranges (interquartile ranges) for major VOCs under both high- and low-NO$_x$ conditions.

4.2 Factors influencing Cl-SOA formation

4.2.1 [Cl$_2$/VOC]$_0$ ratio and Cl exposure.
Spatially variable Cl atom concentrations exert a decisive influence on SOA formation by governing intermediate product distribution, reaction pathways, and particle generation efficiency. In chamber studies, Cl$_2$ is routinely employed as a photolytic precursor to generate Cl atoms, and the initial [Cl$_2$/VOC] ratio is systematically varied (from 0 to 10) to probe SOA yields and mechanisms across a wide range of Cl atom levels. To date, the Cl-initiated oxidation of anthropogenic toluene[42,135] and anisole[138] as well as biogenic isoprene[116] and D-limonene[134] has been well examined in this framework. Fig. 5 summarizes the SOA yields of these VOCs at various initial [Cl$_2$/VOC]$_0$ ratios. Notably, significant differences in SOA yields were observed between the two toluene experiments. The study by Dhulipala *et al.* was
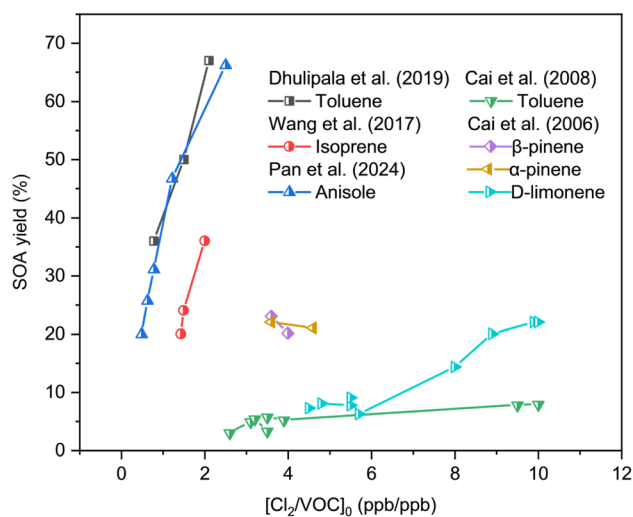

Fig. 5 Influence of [Cl$_2$/VOC]$_0$ on SOA formation from Cl-initiated VOC oxidation. Data are from Dhulipala *et al.* (2019),[135] Cai *et al.* (2008),[42] Wang *et al.* (2017),[116] Pan *et al.* (2024),[138] and Cai *et al.* (2006).[134]

conducted with pre-existing seed aerosol (ammonium sulfate) and higher precursor concentrations, which promoted particle-phase reactions and reduced wall losses, thereby leading to higher SOA yields.[135] In contrast, no seed aerosol was added in the experiments by Cai *et al.*[42] Furthermore, differences in physical structures (*e.g.*, reactor volume and geometry) and detection instruments across smog chambers may introduce uncertainties. The combined effect of these factors resulted in the observed differences in SOA yield for the same precursor.

As shown in Fig. 5, the SOA yields of these VOCs generally increase with increasing [Cl$_2$/VOC]$_0$ ratios. At low [Cl$_2$/VOC]$_0$ ratios, excess precursor leads to insufficient oxidant, causing intermediate accumulation and thus a lower SOA yield. For example, lower [Cl$_2$/VOC]$_0$ ratios ([Cl$_2$/anisole]$_0$ = 0.49, 0.63, and 0.78) in anisole systems promote the formation of gas-phase intermediates like phenol.[138] In this case, insufficient oxidant prevents the conversion of phenol into lower-volatility products. The semi-volatile nature of these intermediates limits their partitioning into the particle phase, resulting in lower SOA yields (20–31.1%). Conversely, at higher [Cl$_2$/VOC]$_0$ ([Cl$_2$/anisole]$_0$ = 2.5), phenol is rapidly generated and consumed, indicating more complete intermediate oxidation and higher SOA yield (66.2%). In addition to intermediates, incomplete precursor consumption also contributes to the lower SOA yields. For instance, D-limonene, with two unsaturated carbon–carbon bonds offering four potential addition sites, was expected to exhibit higher SOA yields than α-pinene and β-pinene. However, under identical initial [Cl$_2$/VOC]$_0$ conditions (3.6–5.5), α-pinene and β-pinene exhibited SOA yields (20.1–23%) nearly triple that of D-limonene (7.2–8%), with the latter achieving expected yields only after doubling its [Cl$_2$/VOC]$_0$ ratio.[134] Furthermore, the [Cl$_2$/VOC]$_0$ ratio indirectly influences SOA chemical composition through reaction kinetics. At low [Cl$_2$/VOC]$_0$ ratios, faster intermediate pathways consume relevant intermediates and Cl atoms, leaving slower intermediate reactions incomplete.[118] The

product distribution resulting from such kinetic competition ultimately governs both the yield and chemical characteristics of SOA. However, with sufficient Cl atoms, nearly all intermediates are converted to lower-volatility products, thereby increasing the SOA yield. Notably, studies have shown that high reaction rates are obtained at high $[Cl_2/VOC]_0$ ratios, suggesting accelerated SOA formation due to elevated oxidant levels.[42,136]

The $[Cl_2/VOC]_0$ ratio has been widely used as a metric for comparing experimental conditions in smog chamber studies, but it fails to account for the influence of key variables such as actual Cl atom concentration, photolysis rate, and reaction time. As a critical parameter in atmospheric chemistry, Cl_{exp} is defined as the product of Cl atom concentration with oxidation time, and it quantifies the cumulative oxidative intensity experienced by VOCs. This enables Cl-SOA yields obtained under different conditions to be uniformly parameterized as a function of atmospheric aging time. For example, calculated Cl_{exp} values in SOA experiments ranged from 5.4×10^9 to 1.6×10^{12} molecules per cm^3 per s, corresponding approximately to 1 day to 10 months of atmospheric oxidation at $[Cl] = 6 \times 10^4$ molecules per cm^3.[143] Therefore, based on the consumption of anisole and reaction time at different $[Cl_2/VOC]_0$ ratios in smog chamber experiments, we have converted the SOA yield into a function of Cl_{exp} (Text S1 and Table S5). Additionally, we have compiled the mass yields of SOA generated in OFRs as a function of Cl_{exp} for key VOCs, including dodecane, toluene, isoprene, α-pinene, and D_5 (Fig. 6a).[107,138,140]

SOA yields indicate that specific precursors generated SOA at yields that were strongly dependent on the oxidant and exposure time. As shown in Fig. 6a, the SOA yields of dodecane, toluene, isoprene, and α-pinene generally increase first and then decrease with the increase in Cl_{exp}, which is consistent with the results in previous studies of OH-initiated oxidation.[144,145] This is mainly attributed to the competing mechanisms of functionalization and fragmentation at different Cl_{exp} levels.[146] At lower Cl_{exp} levels, functionalization dominates, enhancing the degree of oxidation and generating substantial amounts of low-volatility products, thereby driving the increase in SOA yield. As Cl_{exp} levels further increase, fragmentation gradually becomes dominant, leading to the C–C bond cleavage

and the generation of more volatile molecules, ultimately resulting in a decrease in the SOA yield.[140,147] Notably, unlike Cl-SOA generated from other precursors, the mass concentration of D_5 SOA does not decrease at higher Cl_{exp} due to fragmentation reactions, as the cyclic Si–O backbone of D_5 is mostly retained.[107] Moreover, information about the nature of SOA formation and oxidative aging is provided by the Van Krevelen diagram, which plots the H/C ratio as a function of the O/C ratio (Fig. 6b). As oxidative aging progresses, oxygen-containing functional groups may be added into the carbon skeleton of products, resulting in SOA products with higher O/C ratios than their precursors. Despite differences in precursor structures and oxidation pathways, Cl-initiated aging exhibits a consistent distribution trend in the extent of the oxidation, characterized by a H/C ratio that decreases with increasing O/C.

4.2.2 NO_x level. As a key byproduct of combustion processes, NO_x can be co-emitted with other anthropogenic pollutants into the atmosphere, where it exerts significant influences on SOA formation.[148,149] NO_x concentrations exhibit strong spatial heterogeneity, varying by 1–2 orders of magnitude from clean regions to polluted urban areas. Beyond their pivotal role in tropospheric ozone formation and destruction, NO_x levels directly or indirectly interfere with VOC oxidation initiated by Cl, significantly impacting the SOA mass yield, chemical composition, and physicochemical properties.

Although the influence of NO_x on SOA formation has been extensively studied, complex dependencies lead to notable variations across different systems. A systematic analysis of recent findings (Table 1) reveals that for biogenic VOCs like isoprene[41] and α-pinene,[150] as well as aromatic compounds including 1-methylnaphthalene,[50] m-xylene,[49] toluene,[135] and anisole,[138] the presence of NO_x generally reduces SOA yields. Linear alkanes (e.g., decane) and n-alkylcyclohexanes (e.g., butylcyclohexane) also exhibit declining SOA yields with increasing NO_x, though the extent varies among isomers.[130] In contrast, n-alkylcyclohexanes like hexylcyclohexane, heptylcyclohexane, and octylcyclohexane show an opposite trend.[48] These results demonstrate that NO_x effects on Cl-SOA formation are co-modulated by VOC precursor types, molecular structures of VOCs, and NO_x concentration.

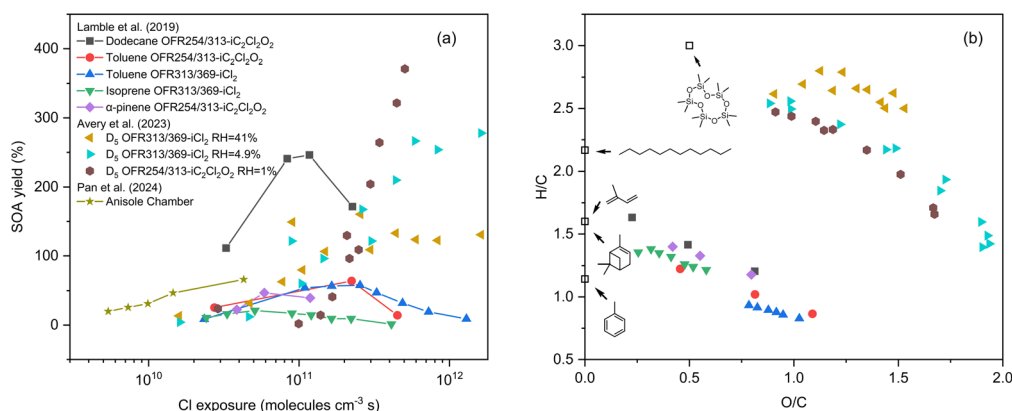**Fig. 6** (a) SOA yields as a function of Cl_{exp} for key VOCs, including dodecane, toluene, isoprene, α-pinene,[140] D_5,[107] and anisole.[138] (b) Van Krevelen diagrams showing the H/C ratio as a function of O/C ratio for SOA generated in OFRs.

Table 1 Influence of NO_x on SOA formation from Cl-initiated VOC oxidation

Precursors	$[VOC]_0$ (ppb)	$[NO_x]_0$ (ppb)	$[Cl_2]_0$ (ppb)	T (K)	RH (%)	Seed	SOA mass ($\mu g\ m^{-3}$)	SOA yield (%)	Notes	References
Isoprene	489	160	200	N/A^a	75	H_2SO_4	76	5.6	The presence	41
	489	0	200	N/A	58	H_2SO_4	97	7.1	of NO_x reduced	
	244	82	100	N/A	45	$(NH_4)_2SO_4$	22	3.2	SOA yields	
	489	0	200	N/A	58	$(NH_4)_2SO_4$	62	4.6		
α-Pinene	15	15	15	298	<5	$(NH_4)_2SO_4$	41	48.0		150
	15	0	15	298	<5	$(NH_4)_2SO_4$	73	85.0		
1-Methylnaphthalene	17	0	45	N/A	N/A	None	55	60.0		50
	17	60	45	N/A	N/A	None	49	55.0		
m-Xylene	78	20	25	298	30	$(NH_4)_2SO_4$	12	4.5		49
	78	<2	25	298	30	$(NH_4)_2SO_4$	24	8.8		
Toluene	39	21	40	N/A	<5	$(NH_4)_2SO_4$	32	22.0		135
	43	<2	40	N/A	<5	$(NH_4)_2SO_4$	53	33.0		
	51	<2	40	N/A	<5	$(NH_4)_2SO_4$	70	36.0		
Anisole	638	231	500	298	<20	None	444	20.7	SOA yields	138
	639	117	500	298	<20	None	456	21.3	decreased	
	626	64	500	298	<20	None	468	22.8	with increasing	
	638	0	500	298	<20	None	581	31.1	NO_x	
Butylcyclohexane	13	36	40	N/A	<5	$(NH_4)_2SO_4$	77	94.0		130
	13	18	40	N/A	<5	$(NH_4)_2SO_4$	92	112.0		
	13	0	40	N/A	<5	$(NH_4)_2SO_4$	140	170.0		
Decane	11	32	40	N/A	<5	$(NH_4)_2SO_4$	59	81.0	The presence	
	11	36	40	N/A	<5	$(NH_4)_2SO_4$	69	95.0	of NO_x reduced	
	11	37	40	N/A	<5	$(NH_4)_2SO_4$	63	86.0	SOA yields	
	11	0	40	N/A	<5	$(NH_4)_2SO_4$	98	134.0		
Hexylcyclohexane	46	210	55–65	298	<5	$(NH_4)_2SO_4$	226	82.6	The presence	48
	44	0	55–65	298	<5	$(NH_4)_2SO_4$	125	48.0	of NO_x increased	
Octylcyclohexane	44	169	55–65	298	<5	$(NH_4)_2SO_4$	362	111.0	SOA yields	
	34	0	55–65	298	<5	$(NH_4)_2SO_4$	243	94.5		
Heptylcyclohexane	45	163	55–65	298	<5	$(NH_4)_2SO_4$	248	88.0		
	38	0	55–65	298	<5	$(NH_4)_2SO_4$	175	72.9		
	37	19	81	N/A	<5	$(NH_4)_2SO_4$	113	82.0		
	22	18	44	N/A	<5	$(NH_4)_2SO_4$	15	17.0		

^{a} N/A: not available.

The dependence of Cl-SOA formation on NO_x levels primarily manifests in altered oxidation conditions and RO_2 radical chemistry. First, NO_x can influence SOA formation by modulating oxidant levels. Without NO_x, secondary OH generation is minimal (OH exposure: 1.5×10^9 molecules per cm^3 per s), whereas Cl_2 + NO experiments exhibit much higher OH exposure (4.3×10^{10} molecules per cm^3 per s).[49] The enhancement of OH is predominantly mediated through the NO_x cycle, where the reaction between NO_x and RO_2 is a secondary OH production pathway.[104] For example, Cl-isoprene simulations indicate that under high-NO_x conditions, up to 40% of isoprene consumption can be attributed to secondary OH chemistry, whereas under low-NO_x conditions, secondary OH contributions are negligible (<0.1%).[41] Similarly, high-NO_x Cl-toluene experiments demonstrate the increased importance of OH chemistry relative to chlorine chemistry.[135] Beyond secondary OH chemistry, high-NO_x conditions also promote O_3 production, indicating that chlorine chemistry can enhance the atmospheric oxidation capacity in the presence of NO_x. Another difference between low- and high-NO_x experiments is the behavior of chlorine species. In high-NO_x environments, Cl-initiated reactions form $ClNO_2$ significantly alter the oxidation

conditions. On the one hand, $ClNO_2$ formation reduces Cl atom concentrations at the beginning of the experiment: simulations of m-xylene experiments showed that cumulative Cl atom exposure under low-NO_x conditions (1.4×10^{10} molecules per cm^3 per s) exceeded that under high-NO_x conditions (8×10^9 molecules per cm^3 per s).[49] On the other hand, $ClNO_2$ serves as a sustained Cl source, with simulated concentrations decreasing after initial formation and stabilizing when UV lights are turned off.[135] In contrast, under low-NO_x conditions, most Cl is converted to HCl, which is relatively stable to photolysis and does not result in significant recycling of Cl. Simultaneously, the low OH concentration in low-NO_x environments hinders HCl from effectively promoting the chlorine cycle through the OH oxidation pathway (OH + HCl $\rightarrow$ Cl + H_2O).

Second, NO significantly alters the fate of RO_2 radicals, which directly determines the volatility of subsequent products and SOA yields. As mentioned in Section 3.3, RO_2 can react with HO_2, RO_2, or NO under certain conditions. Under low-NO_x conditions, RO_2 radicals primarily undergo isomerization/autoxidation and reactions with HO_2 or RO_2 radicals, promoting the formation of low-volatility organic compounds

(including HOMs).[138,150] In high-NO$_x$ environments, the reaction of RO$_2$ with NO primarily forms RO, which favors more volatile oxidation products and increases molecular fragmentation.[50,151] This pathway is further validated by OH oxidation experiments, as H$_2$O$_2$ photolysis-driven oxidation generates abundant HO$_2$, enhances RO$_2$ + HO$_2$ reactions and mitigates NO$_x$ suppression.[49] The fate of RO$_2$ in the gas phase influences particle condensation. Under low-NO$_x$ conditions, the low-volatility organic compounds formed preferentially partition into the particle phase, thereby increasing SOA yields. In contrast, more volatile oxidation products generated under high-NO$_x$ conditions limit SOA formation, consistent with the observed SOA reduction. However, experiments on the Cl-initiated oxidation of the *n*-alkylcyclohexanes revealed that the addition of NO unexpectedly increased HOM yields. This suggests that under high-NO$_x$ conditions, RO may serve as critical intermediates in the autoxidation process of alkanes, promoting the formation of low-volatility products and ultimately leading to increased SOA yields in the presence of NO$_x$.[48,152] These results collectively demonstrate that NO$_x$ dynamically regulates RO$_2$ radical chemistry to influence SOA yields, with net effects depending on synergistic interactions between the VOC molecular structure and the oxidation conditions.

Advances in mass spectrometry have enabled detailed characterization of gas- and particle-phase products from Cl-VOC oxidation under varying NO$_x$ conditions. First, multi-generation observations of Cl-VOC gas-phase products reveal that NO$_x$ appears to delay later-generation product formation. For example, in the anisole system, the ratio of 2-chlorophenol (second-generation product) to phenol (first-generation product) rapidly stabilizes under low-NO$_x$ conditions but shows continuous growth under high-NO$_x$ conditions.[138] This likely occurs because ClNO$_2$ formation in high-NO$_x$ environments slows chemical reactions, with NO$_x$ suppressing the formation rates of typical oxidation products observed under low-NO$_x$ conditions. Second, the influence of NO$_x$ levels on the product distribution follows a consistent pattern across different VOC systems: low-NO$_x$ conditions promote the formation of organic chlorides, whereas high-NO$_x$ conditions favor the production of organic nitrates. Taking the Cl-anisole oxidation as an example, the formation of C$_6$H$_5$OCl increases at lower NO$_x$ levels (63.8 ppb), while the increase in C$_6$H$_5$NO$_3$ becomes more significant at higher NO$_x$ concentrations.[138] Similarly, the gas-phase organic chloride fraction in *m*-xylene decreases from 0.22 (low-NO$_x$) to 0.18 (high-NO$_x$),[49] and isoprene particle-phase chloride contributions decline with increasing NO$_x$ concentrations.[41] Additionally, the O/C ratio range of cycloalkane products under high-NO$_x$ conditions (0.1–1.0) is broader than that under low-NO$_x$ conditions (0.1–0.6), directly explaining higher SOA yields at high NO$_x$.[48]

4.2.3 Relative humidity. RH is one of the critical environmental factors influencing SOA formation. Field studies have demonstrated that during severe haze events, SOA mass concentrations vary with RH.[153,154] Recent findings further reveal complex RH effects on Cl-SOA formation, which can promote, inhibit, or have negligible impacts depending on VOC type and reaction conditions (Fig. 7). For example, increasing
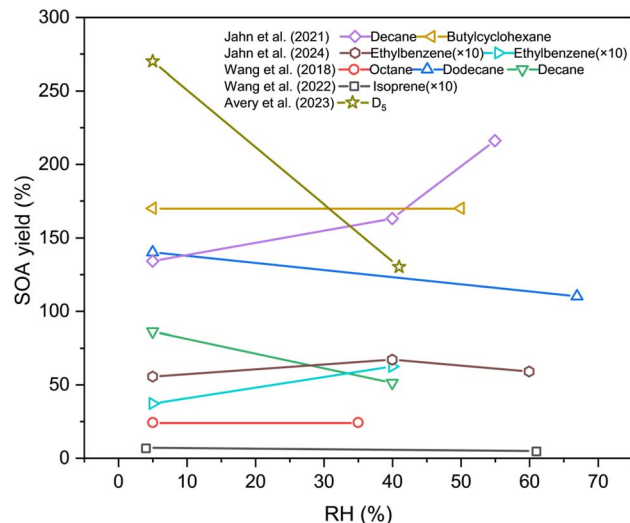
Fig. 7 Influence of RH on SOA formation from Cl-initiated VOC oxidation. Data are from Jahn *et al.* (2021),[130] Jahn *et al.* (2024),[53] Wang *et al.* (2018),[111] Wang *et al.* (2022),[41] and Avery *et al.* (2023).[107]

RH reduces SOA yields for isoprene, dodecane, and D$_5$, but increases yields for ethylbenzene.[53,107] In contrast, SOA yields from butylcyclohexane and octane remain unaffected by RH variations.[111] Notably, decane-SOA yields decrease with high RH under high-NO$_x$ conditions while increasing in the absence of NO$_x$.[130] This opposing trend is attributed to the accelerated hydrolysis of organic nitrates at elevated RH, as previously observed in OH-initiated α-pinene oxidation.[155,156]

The complexity of RH effects stems from its influence on both gas-phase and particle-phase chemistry.[157] In the gas phase, water molecules can directly participate in VOC oxidation by reacting with intermediate products. For example, in Cl-initiated ethylbenzene oxidation, Jahn *et al.* observed that high RH promotes the hydration of gas-phase dicarbonyl compounds, generating more polar diols and carboxylic acids.[53] Given the formation of aerosol liquid water (ALW) through water absorption at high RH, RH further influences particle growth *via* regulating the particle phase state, viscosity, and acidity, which determine the following gas-particle partitioning and particle-phase reactions. For instance, the fraction of C$_{2-5}$ oxygenated compounds in SOA increases from 14% under dry conditions to 19% (40% RH) and 27% (60% RH). This is attributed to ALW that serves as an effective partitioning medium under high-RH conditions, thereby facilitating the absorption and retention of semi-volatile, polar, and water-soluble gaseous products into the particle phase.[53] Conversely, high RH significantly suppresses both organic chloride formation and SOA yields in Cl-initiated alkane oxidation systems. This phenomenon may result from water molecules competitively inhibiting the uptake of key intermediates like 1,4-hydroxycarbonyl compound and DHF, since the addition of Cl to the double bond of DHF is likely the main source of organic chlorides in the process of alkane oxidation.[111] In addition, particle-phase reactions, *e.g.* hemiacetal and acetal reactions could be accelerated in ALW, not only due to its role as aqueous

© 2026 The Author(s). Published by the Royal Society of Chemistry

Environ. Sci.: Atmos., 2026, **6**, 7–26 | 17

reaction media, but also its influences on particle acidity and acid-catalyzed processes in aerosols.[158] During Cl-VOC oxidation, the formation of HCl and organic acids may lower aerosol pH, promoting acid-catalyzed reactions.[130] Cl-initiated isoprene oxidation experiments show high SOA yields under humid conditions when using pre-acidified seed particles. Additionally, water acts as a plasticizer for SOA particles, reducing their viscosity and influencing their growth rates.[159,160] These results demonstrate that RH regulates the reactivity of critical intermediates and their gas-particle partitioning while also influencing the heterogeneous chemistry and oligomerization processes. Thus, its impact on SOA formation is multifaceted and highly dependent on the reaction pathways and product properties of different VOC systems.

5 Conclusions

Significant progress has been made in laboratory and field studies on chlorine chemistry, including the sources and generation mechanisms of atmospheric Cl atoms, the oxidation kinetics of VOCs, and the SOA formation yield and mechanism. This review synthesizes the formation mechanisms of reactive chlorine precursors (Cl_2, $ClNO_2$, HCl, and HOCl) in the atmosphere and their photolytic processes generating Cl atoms. Through analyzing the kinetic characteristics of VOC oxidation initiated by Cl and comparing them with OH radicals, we demonstrate that Cl atoms exhibit reaction rate constants 1–2 orders of magnitude higher than that of OH radicals for most VOCs. Cl-initiated VOC oxidation triggers complex gas-phase reaction chains, with specific pathway differences markedly depending on the compound type. Based on current experimental and theoretical studies, we have identified key missing Cl-initiated pathways for major VOCs within existing chemical mechanisms. As the atmospheric oxidation progresses, the increasing functionalization of oxidation products reduces their vapor pressure, enabling these low-volatility compounds to enter the particle phase through homogeneous nucleation and gas-particle partitioning, thereby forming SOA. Based on current laboratory findings, we typically observe higher SOA yields from Cl-SOA compared to OH-SOA. To bridge laboratory Cl-SOA results with modeling applications, we have developed a parameterization scheme for Cl-SOA yields. This review further examines the influence of key factors on Cl-SOA formation. The $[Cl_2/VOC]_0$ ratio affects SOA yields and the chemical composition by modulating intermediate product distributions, reaction pathways, and the particle formation efficiency. Cl_{exp} can influence SOA yield by regulating the competition between functionalization and fragmentation processes. The presence of NO_x alters the oxidation conditions by generating $ClNO_2$ and secondary OH radicals, while also influencing the fate of RO_2 radicals and the volatility of subsequent products, which ultimately affects SOA yields. RH regulates the availability of water in the reaction system. This water acts as both a reactant and a medium to influence product distributions and SOA formation processes.

Despite the abovementioned advances in Cl-associated chemistry, the research in this field is far from complete, and

several critical issues remain unresolved. Future studies should prioritize the following areas:

(1) Current research in modeling reactive chlorine formation has made significant progress, with kinetic parameters for major gas-phase reactions and photolysis processes becoming well established, while heterogeneous $ClNO_2$ chemistry has been successfully implemented in the model.[161,162] However, existing models still face substantial challenges in simulating key reactive chlorine species such as Cl_2 and HOCl, primarily due to insufficient parameterization of kinetic parameters in their heterogeneous reaction mechanisms, which hinders the accurate source quantification and reliable reproduction of observed concentrations. Future efforts should focus on integrating multi-environment field observations with laboratory studies to better constrain the kinetic parameters for heterogeneous reactions, thereby systematically improving the capability of the predictive model for spatiotemporal distribution of reactive chlorine.

(2) To ensure analytical accuracy in instrumental measurements, many laboratory studies use the VOC precursor and oxidant concentrations significantly higher than respective ambient levels. This may alter the key reaction pathways of RO_2, affect aerosol nucleation and growth mechanisms, and lead to uncertainties in SOA yields. Therefore, further development of online high-time-resolution mass spectrometry is required to maintain high-sensitivity identification and accurate quantification of reaction intermediates and products under simulation conditions approaching realistic atmospheric concentration levels. Concurrently, experimental designs should ensure that environmental parameters such as RH, NO_x levels, and particle acidity remain consistent with actual atmospheric conditions. Such improvements will enhance the reliability of experimental data and provide a more accurate foundation for model parameterization.

(3) As mentioned above, Cl-SOA generated in the laboratory is produced by a single precursor, and the formation and physicochemical properties of Cl-SOA in VOC mixtures remain poorly understood. Given the widespread presence of diverse biogenic and anthropogenic volatile organic compounds in the real atmospheric environment, these compounds can undergo natural mixing through atmospheric transport and collectively participate in SOA formation *via* atmospheric oxidation processes. Therefore, the observed SOA concentrations cannot be adequately explained solely by the contribution of individual precursors; instead, it is essential to account for potential synergistic or inhibitory interactions among mixed VOCs. Numerous laboratory studies have been conducted on OH-driven oxidation of mixed VOCs,[163–165] whereas the formation mechanisms of Cl-SOA still require further validation under more complex gas-phase mixture systems.

(4) As detailed in Section 3.3, current chemical mechanisms (MCM) lack explicit oxidation pathways and kinetic parameters for Cl-initiated reactions beyond alkanes. In updated reaction mechanisms, only peroxyl radicals formed in the first-generation reaction associated with Cl atoms have been considered. Given the increasing concentrations of reactive chlorine species and the characteristically high reactivity and

18 | *Environ. Sci.: Atmos.*, 2026, **6**, 7–26

© 2026 The Author(s). Published by the Royal Society of Chemistry

yield of chlorine chemistry, developing detailed mechanisms of chlorine chemistry is crucial for a more accurate representation by current models. Thus, future efforts should prioritize establishing kinetic parameters and oxidation pathways for VOC degradation induced by Cl atoms through laboratory studies, as well as theoretical calculations.

(5) Integrating laboratory-derived Cl-SOA yield data into chemical models helps reduce current model biases.[21] However, due to the scarcity of experimental data and the wide distribution range of existing yield values, the most substantial uncertainties of the current study are introduced by the parametrizations of SOA yields. Therefore, more experimental studies are needed to reduce the uncertainties in Cl-SOA formation. To further improve and constrain SOA simulations, it is essential to clarify the specific parametric requirements for Cl-SOA yield in chemical transport models, including environmental conditions (*e.g.*, NO_x levels and Cl_{exp}) and applicable numerical ranges.

Author contributions

Yinghong Sun: conceptualization, methodology, investigation, formal analysis, writing – original draft, writing – review & editing. Li Xu: writing – review & editing. Jianlong Li: writing – review & editing. Kun Li: writing – review & editing. Narcisse Tsona Tchinda: writing – review & editing. Lin Du: conceptualization, supervision, funding acquisition, writing – review & editing.

Conflicts of interest

There are no conflicts of interest to declare.

Data availability

The review synthesizes information from previously published studies, as cited in the text.

Supplementary information: estimation of Cl exposure, statistics of reaction rate constants between organic compounds and Cl atoms, key missing pathways of Cl-initiated oxidation in chemical mechanisms, comparison of SOA yields from oxidation by Cl atoms *versus* OH radicals, and parameterization of Cl-SOA yields. See DOI: **https://doi.org/10.1039/d5ea00101c**.

Acknowledgements

References

1 Q. Zhang, Y. Zheng, D. Tong, M. Shao, S. Wang, Y. Zhang, X. Xu, J. Wang, H. He, W. Liu, Y. Ding, Y. Lei, J. Li, Z. Wang, X. Zhang, Y. Wang, J. Cheng, Y. Liu, Q. Shi, L. Yan, G. Geng, C. Hong, M. Li, F. Liu, B. Zheng, J. Cao, A. Ding, J. Gao, Q. Fu, J. Huo, B. Liu, Z. Liu, F. Yang, K. He and J. Hao, Drivers of improved $PM_{2.5}$ air quality in China from 2013 to 2017, *Proc. Natl. Acad. Sci. U. S. A.*, 2019, **116**, 24463–24469.

2 J. S. Apte, M. Brauer, A. J. Cohen, M. Ezzati and C. A. Pope, Ambient $PM_{2.5}$ Reduces Global and Regional Life Expectancy, *Environ. Sci. Technol. Lett.*, 2018, **5**, 546–551.

3 N. Bellouin, J. Quaas, E. Gryspeerdt, S. Kinne, P. Stier, D. Watson-Parris, O. Boucher, K. S. Carslaw, M. Christensen, A. L. Daniau, J. L. Dufresne, G. Feingold, S. Fiedler, P. Forster, A. Gettelman, J. M. Haywood, U. Lohmann, F. Malavelle, T. Mauritsen, D. T. McCoy, G. Myhre, J. Mülmenstädt, D. Neubauer, A. Possner, M. Rugenstein, Y. Sato, M. Schulz, S. E. Schwartz, O. Sourdeval, T. Storelvmo, V. Toll, D. Winker and B. Stevens, Bounding Global Aerosol Radiative Forcing of Climate Change, *Rev. Geophys.*, 2020, **58**, e2019RG000660.

4 M. Shrivastava, C. D. Cappa, J. Fan, A. H. Goldstein, A. B. Guenther, J. L. Jimenez, C. Kuang, A. Laskin, S. T. Martin, N. L. Ng, T. Petaja, J. R. Pierce, P. J. Rasch, P. Roldin, J. H. Seinfeld, J. Shilling, J. N. Smith, J. A. Thornton, R. Volkamer, J. Wang, D. R. Worsnop, R. A. Zaveri, A. Zelenyuk and Q. Zhang, Recent advances in understanding secondary organic aerosol: Implications for global climate forcing, *Rev. Geophys.*, 2017, **55**, 509–559.

5 J. S. Apte, J. D. Marshall, A. J. Cohen and M. Brauer, Addressing Global Mortality from Ambient $PM_{2.5}$, *Environ. Sci. Technol.*, 2015, **49**, 8057–8066.

6 R.-J. Huang, Y. Zhang, C. Bozzetti, K.-F. Ho, J.-J. Cao, Y. Han, K. R. Daellenbach, J. G. Slowik, S. M. Platt, F. Canonaco, P. Zotter, R. Wolf, S. M. Pieber, E. A. Bruns, M. Crippa, G. Ciarelli, A. Piazzalunga, M. Schwikowski, G. Abbaszade, J. Schnelle-Kreis, R. Zimmermann, Z. An, S. Szidat, U. Baltensperger, I. El Haddad and A. S. H. Prevot, High secondary aerosol contribution to particulate pollution during haze events in China, *Nature*, 2014, **514**, 218–222.

7 T. Chen, J. Liu, Y. Liu, Q. Ma, Y. Ge, C. Zhong, H. Jiang, B. Chu, P. Zhang, J. Ma, P. Liu, Y. Wang, Y. Mu and H. He, Chemical characterization of submicron aerosol in summertime Beijing: A case study in southern suburbs in 2018, *Chemosphere*, 2020, **247**, 125918.

8 X. Huang, H. Yun, Z. Gong, X. Li, L. He, Y. Zhang and M. Hu, Source apportionment and secondary organic aerosol estimation of $PM_{2.5}$ in an urban atmosphere in China, *Sci. China Earth Sci.*, 2014, **57**, 1352–1362.

9 P. K. H. Lee, J. R. Brook, E. Dabek-Zlotorzynska and S. A. Mabury, Identification of the major sources contributing to $PM_{2.5}$ observed in Toronto, *Environ. Sci. Technol.*, 2003, **37**, 4831–4840.

10 V. F. McNeill, Aqueous Organic Chemistry in the Atmosphere: Sources and Chemical Processing of Organic Aerosols, *Environ. Sci. Technol.*, 2015, **49**, 1237–1244.

11 D. Srivastava, T. V. Vu, S. Tong, Z. Shi and R. M. Harrison, Formation of secondary organic aerosols from anthropogenic precursors in laboratory studies, *npj Clim. Atmos. Sci.*, 2022, **5**, 1–30.

© 2026 The Author(s). Published by the Royal Society of Chemistry

Environ. Sci.: Atmos., 2026, **6**, 7–26 | 19

12 T. Berndt, S. Richters, T. Jokinen, N. Hyttinen, T. Kurtén, R. V. Otkjær, H. G. Kjaergaard, F. Stratmann, H. Herrmann, M. Sipilä, M. Kulmala and M. Ehn, Hydroxyl radical-induced formation of highly oxidized organic compounds, *Nat. Commun.*, 2016, **7**, 13677.

13 M. Sarrafzadeh, J. Wildt, I. Pullinen, M. Springer, E. Kleist, R. Tillmann, S. H. Schmitt, C. Wu, T. F. Mentel, D. Zhao, D. R. Hastie and A. Kiendler-Scharr, Impact of NOx and OH on secondary organic aerosol formation from β-pinene photooxidation, *Atmos. Chem. Phys.*, 2016, **16**, 11237–11248.

14 H. Shen, L. Vereecken, S. Kang, I. Pullinen, H. Fuchs, D. Zhao and T. F. Mentel, Unexpected significance of a minor reaction pathway in daytime formation of biogenic highly oxygenated organic compounds, *Sci. Adv.*, 2022, **8**, 2375–2548.

15 S. Iyer, M. P. Rissanen, R. Valiev, S. Barua, J. E. Krechmer, J. Thornton, M. Ehn and T. Kurtén, Molecular mechanism for rapid autoxidation in α-pinene ozonolysis, *Nat. Commun.*, 2021, **12**, 878.

16 S. Nikkho, B. Bai, F. Mahrt, J. Zaks, L. Peng, K. J. Kiland, P. Liu and A. K. Bertram, Secondary Organic Aerosol from Biomass Burning Phenolic Compounds and Nitrate Radicals can be Highly Viscous over a Wide Relative Humidity Range, *Environ. Sci. Technol.*, 2024, **58**, 21702–21715.

17 K. H. Bates, G. J. P. Burke, J. D. Cope and T. B. Nguyen, Secondary organic aerosol and organic nitrogen yields from the nitrate radical (NO_3) oxidation of alpha-pinene from various RO_2 fates, *Atmos. Chem. Phys.*, 2022, **22**, 1467–1482.

18 X. Peng, T. Wang, W. Wang, A. R. Ravishankara, C. George, M. Xia, M. Cai, Q. Li, C. M. Salvador, C. Lau, X. Lyu, C. N. Poon, A. Mellouki, Y. Mu, M. Hallquist, A. Saiz-Lopez, H. Guo, H. Herrmann, C. Yu, J. Dai, Y. Wang, X. Wang, A. Yu, K. Leung, S. Lee and J. Chen, Photodissociation of particulate nitrate as a source of daytime tropospheric Cl_2, *Nat. Commun.*, 2022, **13**, 939.

19 M. Priestley, M. le Breton, T. J. Bannan, S. D. Worrall, A. Bacak, A. R. D. Smedley, E. Reyes-Villegas, A. Mehra, J. Allan, A. R. Webb, D. E. Shallcross, H. Coe and C. J. Percival, Observations of organic and inorganic chlorinated compounds and their contribution to chlorine radical concentrations in an urban environment in northern Europe during the wintertime, *Atmos. Chem. Phys.*, 2018, **18**, 13481–13493.

20 Q. Li, X. Fu, X. Peng, W. Wang, A. Badia, R. P. Fernandez, C. A. Cuevas, Y. Mu, J. Chen, J. L. Jimenez, T. Wang and A. Saiz-Lopez, Halogens Enhance Haze Pollution in China, *Environ. Sci. Technol.*, 2021, **55**, 13625–13637.

21 X. Liu, L. Liu, B. Zhang, P. Liu, R.-J. Huang, L. Hildebrandt Ruiz, R. Miao, Q. Chen and X. Wang, Modeling the Global Impact of Chlorine Chemistry on Secondary Organic Aerosols, *Environ. Sci. Technol.*, 2024, **58**, 23064–23074.

22 M. S. Choi, X. Qiu, J. Zhang, S. Wang, X. Li, Y. Sun, J. Chen and Q. Ying, Study of Secondary Organic Aerosol Formation from Chlorine Radical-Initiated Oxidation of Volatile Organic Compounds in a Polluted Atmosphere Using a 3D Chemical Transport Model, *Environ. Sci. Technol.*, 2020, **54**, 13409–13418.

23 G. Chen, X. Fan, Z. Lin, X. Ji, Z. Chen, L. Xu and J. Chen, Driving factors and photochemical impacts of Cl_2 in coastal atmosphere of Southeast China, *npj Clim. Atmos. Sci.*, 2025, **8**, 135.

24 S. Yin, X. Yi, L. Li, L. Huang, M. C. G. Ooi, Y. Wang, D. T. Allen and D. G. Streets, An Updated Anthropogenic Emission Inventory of Reactive Chlorine Precursors in China, *ACS Earth Space Chem.*, 2022, **6**, 1846–1857.

25 X. Fu, T. Wang, S. Wang, L. Zhang, S. Cai, J. Xing and J. Hao, Anthropogenic Emissions of Hydrogen Chloride and Fine Particulate Chloride in China, *Environ. Sci. Technol.*, 2018, **52**, 1644–1654.

26 X. Yi, S. Yin, L. Huang, H. Li, Y. Wang, Q. Wang, A. Chan, D. Traoré, M. C. G. Ooi, Y. Chen, D. T. Allen and L. Li, Anthropogenic emissions of atomic chlorine precursors in the Yangtze River Delta region, China, *Sci. Total Environ.*, 2021, **771**, 144644.

27 Z. Ding, S. Tian, J. Dang and Q. Zhang, New mechanistic understanding for atmospheric oxidation of isoprene initiated by atomic chlorine, *Sci. Total Environ.*, 2021, **801**, 149768.

28 L. Wang, J. Arey and R. Atkinson, Reactions of chlorine atoms with a series of aromatic hydrocarbons, *Environ. Sci. Technol.*, 2005, **39**, 5302–5310.

29 M. Antiñolo, M. Asensio, J. Albaladejo and E. Jiménez, Gas-Phase Reaction of trans-2-Methyl-2-butenal with Cl: Kinetics, Gaseous Products, and SOA Formation, *Atmosphere*, 2020, **11**, 715.

30 A. Rodríguez, D. Rodríguez, A. Garzón, A. Soto, A. Aranda and A. Notario, Kinetics and mechanism of the atmospheric reactions of atomic chlorine with 1-penten-3-ol and (Z)-2-penten-1-ol: an experimental and theoretical study, *Phys. Chem. Chem. Phys.*, 2010, **12**, 12245–12258.

31 K. Han, H. Liu, C. Yin, Y. Zhao and S. Bi, Mechanistic and kinetics study on the reaction of methylallyl alcohol with Cl: A theoretical study, *J. Chem. Theor. Comput.*, 2021, **1204**, 113388.

32 R. Atkinson, D. Baulch, R. Cox, J. Crowley, R. Hampson, R. Hynes, M. Jenkin, M. Rossi, J. Troe and I. Subcommittee, Evaluated kinetic and photochemical data for atmospheric chemistry: Volume II–gas phase reactions of organic species, *Atmos. Chem. Phys.*, 2006, **6**, 3625–4055.

33 T. J. Wallington, L. M. Skewes and W. O. Siegl, Kinetics of the gas phase reaction of chlorine atoms with a series of alkenes, alkynes and aromatic species at 295 K, *J. Photochem. Photobiol., A*, 1988, **45**, 167–175.

34 A. Lauraguais, I. Bejan, I. Barnes, P. Wiesen, C. Coeur-Tourneur and A. Cassez, Rate Coefficients for the Gas-Phase Reaction of Chlorine Atoms with a Series of Methoxylated Aromatic Compounds, *J. Phys. Chem. A*, 2014, **118**, 1777–1784.

35 M. Riva, R. M. Healy, P.-M. Flaud, E. Perraudin, J. C. Wenger and E. Villenave, Kinetics of the Gas-Phase Reactions of

Chlorine Atoms with Naphthalene, Acenaphthene, and Acenaphthylene, *J. Phys. Chem. A*, 2014, **118**, 3535–3540.

36 G. Thiault, A. Mellouki and G. Le Bras, Kinetics of gas phase reactions of OH and Cl with aromatic aldehydes, *Phys. Chem. Chem. Phys.*, 2002, **4**, 2194–2199.

37 O. W. Wingenter, D. R. Blake, N. J. Blake, B. C. Sive, F. S. Rowland, E. Atlas and F. Flocke, Tropospheric hydroxyl and atomic chlorine concentrations, and mixing timescales determined from hydrocarbon and halocarbon measurements made over the Southern Ocean, *J. Geophys. Res. Atmos.*, 1999, **104**, 21819–21828.

38 A. Saiz-Lopez and R. von Glasow, Reactive halogen chemistry in the troposphere, *Chem. Soc. Rev.*, 2012, **41**, 6448–6472.

39 O. W. Wingenter, B. C. Sive, N. J. Blake, D. R. Blake and F. S. Rowland, Atomic chlorine concentrations derived from ethane and hydroxyl measurements over the equatorial Pacific Ocean: Implication for dimethyl sulfide and bromine monoxide, *J. Geophys. Res. Atmos.*, 2005, **110**, 308.

40 M. Riva, R. M. Healy, P.-M. Flaud, E. Perraudin, J. C. Wenger and E. Villenave, Gas- and Particle-Phase Products from the Chlorine-Initiated Oxidation of Polycyclic Aromatic Hydrocarbons, *J. Phys. Chem. A*, 2015, **119**, 11170–11181.

41 D. S. Wang, C. G. Masoud, M. Modi and L. Hildebrandt Ruiz, Isoprene–Chlorine Oxidation in the Presence of NOx and Implications for Urban Atmospheric Chemistry, *Environ. Sci. Technol.*, 2022, **56**, 9251–9264.

42 X. Cai, L. D. Ziemba and R. J. Griffin, Secondary aerosol formation from the oxidation of toluene by chlorine atoms, *Atmos. Environ.*, 2008, **42**, 7348–7359.

43 Y. J. Tham, Z. Wang, Q. Li, H. Yun, W. Wang, X. Wang, L. Xue, K. Lu, N. Ma, B. Bohn, X. Li, S. Kecorius, J. Größ, M. Shao, A. Wiedensohler, Y. Zhang and T. Wang, Significant concentrations of nitryl chloride sustained in the morning: investigations of the causes and impacts on ozone production in a polluted region of northern China, *Atmos. Chem. Phys.*, 2016, **16**, 14959–14977.

44 W. Ma, Z. Feng, X. Chen, M. Xia, Y. Liu, Y. Zhang, Y. Liu, Y. Wang, F. Zheng, C. Hua, J. Li, Z. Zhao, H. Yang, M. Kulmala, D. R. Worsnop, H. He and Y. Liu, Overlooked Significance of Reactive Chlorines in the Reacted Loss of VOCs and the Formation of O_3 and SOA, *Environ. Sci. Technol.*, 2025, **59**, 6155–6166.

45 X. Wang, D. J. Jacob, X. Fu, T. Wang, M. L. Breton, M. Hallquist, Z. Liu, E. E. McDuffie and H. Liao, Effects of Anthropogenic Chlorine on $PM_{2.5}$ and Ozone Air Quality in China, *Environ. Sci. Technol.*, 2020, **54**, 9908–9916.

46 W. Ma, X. Chen, M. Xia, Y. Liu, Y. Wang, Y. Zhang, F. Zheng, J. Zhan, C. Hua, Z. Wang, W. Wang, P. Fu, M. Kulmala and Y. Liu, Reactive Chlorine Species Advancing the Atmospheric Oxidation Capacities of Inland Urban Environments, *Environ. Sci. Technol.*, 2023, **57**, 14638–14647.

47 G. Chen, L. Xu, S. Yu, L. Xue, Z. Lin, C. Yang, X. Ji, X. Fan, Y. J. Tham, H. Wang, Y. Hong, M. Li, J. H. Seinfeld and J. Chen, Increasing Contribution of Chlorine Chemistry to

Wintertime Ozone Formation Promoted by Enhanced Nitrogen Chemistry, *Environ. Sci. Technol.*, 2024, **58**, 22714–22721.

48 K. Wang, W. Wang, C. Fan, J. Li, T. Lei, W. Zhang, B. Shi, Y. Chen, M. Liu, C. Lian, Z. Wang and M. Ge, Reactions of C_{12}–C_{14} n-Alkylcyclohexanes with Cl Atoms: Kinetics and Secondary Organic Aerosol Formation, *Environ. Sci. Technol.*, 2022, **56**, 4859–4870.

49 N. Bhattacharyya, M. Modi, L. G. Jahn and L. Hildebrandt Ruiz, Different chlorine and hydroxyl radical environments impact m-xylene oxidation products, *Environ. Sci.: Atmos.*, 2023, **3**, 1174–1185.

50 X. Wang, W. Wang, C. Hou, C. Fan, T. Lei, J. Li and M. Ge, Secondary organic aerosols from oxidation of 1-methylnaphthalene: Yield, composition, and volatility, *Sci. Total Environ.*, 2024, **918**, 170379.

51 X. Peng, W. Wang, M. Xia, H. Chen, A. R. Ravishankara, Q. Li, A. Saiz-Lopez, P. Liu, F. Zhang, C. Zhang, L. Xue, X. Wang, C. George, J. Wang, Y. Mu, J. Chen and T. Wang, An unexpected large continental source of reactive bromine and chlorine with significant impact on wintertime air quality, *Natl. Sci. Rev.*, 2021, **8**, nwaa304.

52 J. J. Orlando, G. S. Tyndall, E. C. Apel, D. D. Riemer and S. E. Paulson, Rate coefficients and mechanisms of the reaction of Cl-atoms with a series of unsaturated hydrocarbons under atmospheric conditions, *Int. J. Chem. Kinet.*, 2003, **35**, 334–353.

53 L. G. Jahn, K. N. McPherson and L. Hildebrandt Ruiz, Effects of Relative Humidity and Photoaging on the Formation, Composition, and Aging of Ethylbenzene SOA: Insights from Chamber Experiments on Chlorine Radical-Initiated Oxidation of Ethylbenzene, *ACS Earth Space Chem.*, 2024, **8**, 675–688.

54 C. Fan, W. Wang, K. Wang, T. Lei, W. Xiang, C. Hou, J. Li, Y. Guo and M. Ge, Temperature effects on SOA formation of n-dodecane reaction initiated by Cl atoms, *Atmos. Environ.*, 2025, **346**, 121070.

55 C. Wang, J. Liggio, J. J. B. Wentzell, S. Jorga, A. Folkerson and J. P. D. Abbatt, Chloramines as an important photochemical source of chlorine atoms in the urban atmosphere, *Proc. Natl. Acad. Sci. U. S. A.*, 2023, **120**, e2220889120.

56 J. M. Mattila, P. S. J. Lakey, M. Shiraiwa, C. Wang, J. P. D. Abbatt, C. Arata, A. H. Goldstein, L. Ampollini, E. F. Katz, P. F. DeCarlo, S. Zhou, T. F. Kahan, F. J. Cardoso-Saldaña, L. H. Ruiz, A. Abeleira, E. K. Boedicker, M. E. Vance and D. K. Farmer, Multiphase Chemistry Controls Inorganic Chlorinated and Nitrogenated Compounds in Indoor Air during Bleach Cleaning, *Environ. Sci. Technol.*, 2020, **54**, 1730–1739.

57 C. B. Faxon, S. V. Dhulipala, D. T. Allen and L. Hildebrandt Ruiz, Heterogeneous production of Cl_2 from particulate chloride: Effects of composition and relative humidity, *AIChE J.*, 2018, **64**, 3151–3158.

58 F.-P. B. J, M. J. Ezell and J. N. Pitts, Formation of Chemically Active Chlorine Compounds by Reactions of Atmospheric

© 2026 The Author(s). Published by the Royal Society of Chemistry

Environ. Sci.: Atmos., 2026, **6**, 7–26 | 21

NaCl Particles with Gaseous N_2O_5 and $ClONO_2$, *Nature*, 1989, **337**, 241–244.

59 M. Le Breton, Å. M. Hallquist, R. K. Pathak, D. Simpson, Y. Wang, J. Johansson, J. Zheng, Y. Yang, D. Shang, H. Wang, Q. Liu, C. Chan, T. Wang, T. J. Bannan, M. Priestley, C. J. Percival, D. E. Shallcross, K. Lu, S. Guo, M. Hu and M. Hallquist, Chlorine oxidation of VOCs at a semi-rural site in Beijing: significant chlorine liberation from $ClNO_2$ and subsequent gas- and particle-phase Cl–VOC production, *Atmos. Chem. Phys.*, 2018, **18**, 13013–13030.

60 A. T. Ahern, L. Goldberger, L. Jahl, J. Thornton and R. C. Sullivan, Production of N_2O_5 and $ClNO_2$ through Nocturnal Processing of Biomass-Burning Aerosol, *Environ. Sci. Technol.*, 2017, **52**, 550–559.

61 T. Wang, Y. J. Tham, L. Xue, Q. Li, Q. Zha, Z. Wang, S. C. Poon, W. P. Dubé, D. R. Blake and P. K. Louie, Observations of nitryl chloride and modeling its source and effect on ozone in the planetary boundary layer of southern China, *J. Geophys. Res. Atmos.*, 2016, **121**, 2476–2489.

62 W. Zhang, J. Zhong, R. Li, L. Li, X. Ma, Y. Ji, G. Li, J. S. Francisco and T. An, Distinctive Heterogeneous Reaction Mechanism of $ClNO_2$ on the Air–Water Surface Containing Cl, *J. Am. Chem. Soc.*, 2023, **145**, 22649–22658.

63 C. Yan, Y. J. Tham, W. Nie, M. Xia, H. Wang, Y. Guo, W. Ma, J. Zhan, C. Hua, Y. Li, C. Deng, Y. Li, F. Zheng, X. Chen, Q. Li, G. Zhang, A. S. Mahajan, C. A. Cuevas, D. D. Huang, Z. Wang, Y. Sun, A. Saiz-Lopez, F. Bianchi, V.-M. Kerminen, D. R. Worsnop, N. M. Donahue, J. Jiang, Y. Liu, A. Ding and M. Kulmala, Increasing contribution of nighttime nitrogen chemistry to wintertime haze formation in Beijing observed during COVID-19 lockdowns, *Nat. Geosci.*, 2023, **16**, 975–981.

64 K. D. Custard, K. A. Pratt, S. Wang and P. B. Shepson, Constraints on Arctic Atmospheric Chlorine Production through Measurements and Simulations of Cl_2 and ClO, *Environ. Sci. Technol.*, 2016, **50**, 12394–12400.

65 X. Liu, H. Qu, L. G. Huey, Y. Wang, S. Sjostedt, L. Zeng, K. Lu, Y. Wu, M. Hu, M. Shao, T. Zhu and Y. Zhang, High Levels of Daytime Molecular Chlorine and Nitryl Chloride at a Rural Site on the North China Plain, *Environ. Sci. Technol.*, 2017, **51**, 9588–9595.

66 J. M. Roberts, H. D. Osthoff, S. S. Brown and A. R. Ravishankara, N_2O_5 oxidizes chloride to Cl_2 in acidic atmospheric aerosol, *Science*, 2008, **321**, 1059.

67 E. M. Knipping and D. Dabdub, Impact of chlorine emissions from sea-salt aerosol on coastal urban ozone, *Environ. Sci. Technol.*, 2003, **37**, 275–284.

68 M. J. Lawler, R. Sander, L. J. Carpenter, J. D. Lee, R. von Glasow, R. Sommariva and E. S. Saltzman, HOCl and Cl_2 observations in marine air, *Atmos. Chem. Phys.*, 2011, **11**, 7617–7628.

69 Q. Chen, M. Xia, X. Peng, C. Yu, P. Sun, Y. Li, Y. Liu, Z. Xu, Z. Xu, R. Wu, W. Nie, A. Ding, Y. Zhao and T. Wang, Large Daytime Molecular Chlorine Missing Source at a Suburban Site in East China, *J. Geophys. Res. Atmos.*, 2022, **127**, e2021JD035796.

70 M. Xia, X. Peng, W. Wang, C. Yu, P. Sun, Y. Li, Y. Liu, Z. Xu, Z. Wang, Z. Xu, W. Nie, A. Ding and T. Wang, Significant production of $ClNO_2$ and possible source of Cl_2 from N_2O_5 uptake at a suburban site in eastern China, *Atmos. Chem. Phys.*, 2020, **20**, 6147–6158.

71 J. Liao, L. G. Huey, Z. Liu, D. J. Tanner, C. A. Cantrell, J. J. Orlando, F. M. Flocke, P. B. Shepson, A. J. Weinheimer, S. R. Hall, K. Ullmann, H. J. Beine, Y. Wang, E. D. Ingall, C. R. Stephens, R. S. Hornbrook, E. C. Apel, D. Riemer, A. Fried, R. L. Mauldin, J. N. Smith, R. M. Staebler, J. A. Neuman and J. B. Nowak, High levels of molecular chlorine in the Arctic atmosphere, *Nat. Geosci.*, 2014, **7**, 91–94.

72 K. W. Oum, M. J. Lakin, D. O. DeHaan, T. Brauers and B. J. Finlayson-Pitts, Formation of molecular chlorine from the photolysis of ozone and aqueous sea-salt particles, *Science*, 1998, **279**, 74–77.

73 E. M. Knipping and D. Dabdub, Modeling Cl_2 formation from aqueous NaCl particles: Evidence for interfacial reactions and importance of Cl_2 decomposition in alkaline solution, *J. Geophys. Res. Atmos.*, 2002, **107**, 30.

74 Q. Chen, X. Wang, X. Fu, X. Li, B. Alexander, X. Peng, W. Wang, M. Xia, Y. Tan, J. Gao, J. Chen, Y. Mu, P. Liu and T. Wang, Impact of Molecular Chlorine Production from Aerosol Iron Photochemistry on Atmospheric Oxidative Capacity in North China, *Environ. Sci. Technol.*, 2024, **58**, 12585–12597.

75 M. M. J. W. van Herpen, Q. Li, A. Saiz-Lopez, J. B. Liisberg, T. Roeckmann, C. A. Cuevas, R. P. Fernandez, J. E. Mak, N. M. Mahowald, P. Hess, D. Meidan, J.-B. W. Stuut and M. S. Johnson, Photocatalytic chlorine atom production on mineral dust-sea spray aerosols over the North Atlantic, *Proc. Natl. Acad. Sci. U. S. A.*, 2023, **120**, e2303974120.

76 J. Mack and J. R. Bolton, Photochemistry of nitrite and nitrate in aqueous solution: a review, *J. Photochem. Photobiol., A*, 1999, **128**, 1–13.

77 R. Zellner, M. Exner and H. Herrmann, Absolute OH quantum yields in the laser photolysis of nitrate, nitrite and dissolved H_2O_2 at 308 and 351 nm in the temperature range 278–353 K, *J. Atmos. Chem.*, 1990, **10**, 411–425.

78 T. X. Wang and D. W. Margerum, Kinetics of reversible chlorine hydrolysis: temperature dependence and general-acid/base-assisted mechanisms, *Inorg. Chem.*, 1994, **33**, 1050–1055.

79 E. Z. Dalton, E. H. Hoffmann, T. Schaefer, A. Tilgner, H. Herrmann and J. D. Raff, Daytime Atmospheric Halogen Cycling through Aqueous-Phase Oxygen Atom Chemistry, *J. Am. Chem. Soc.*, 2023, **145**, 15652–15657.

80 D. W. Johnson and D. W. Margerum, Non-metal redox kinetics: a reexamination of the mechanism of the reaction between hypochlorite and nitrite ions, *Inorg. Chem.*, 1991, **30**, 4845–4851.

81 G. Chen, X. Fan, S. Yu, Y. J. Tham, Z. Lin, X. Ji, L. Xu and J. Chen, HOCl Formation Driven by Photochemical Processes Enhanced Atmospheric Oxidation Capacity in a Coastal Atmosphere, *Environ. Sci. Technol.*, 2025, **59**, 5164–5171.

82 S. M. McNamara, A. R. W. Raso, S. Wang, S. Thanekar, E. J. Boone, K. R. Kolesar, P. K. Peterson, W. R. Simpson, J. D. Fuentes, P. B. Shepson and K. A. Pratt, Springtime Nitrogen Oxide-Influenced Chlorine Chemistry in the Coastal Arctic, *Environ. Sci. Technol.*, 2019, **53**, 8057–8067.

83 M. J. Molina, T. L. Tso, L. T. Molina and F. C. Y. Wang, Antarctic Stratospheric Chemistry of Chlorine Nitrate, Hydrogen Chloride, and Ice: Release of Active Chlorine, *Science*, 1987, **238**, 1253–1257.

84 S. Pechtl and R. von Glasow, Reactive chlorine in the marine boundary layer in the outflow of polluted continental air: A model study, *Geophys. Res. Lett.*, 2007, **34**, L11813.

85 C. W. Spicer, E. G. Chapman, B. J. Finlayson-Pitts, R. A. Plastridge, J. M. Hubbe, J. D. Fast and C. M. Berkowitz, Unexpectedly high concentrations of molecular chlorine in coastal air, *Nature*, 1998, **394**, 353–356.

86 O. W. Wingenter, M. K. Kubo, N. J. Blake, T. W. Smith, D. R. Blake and F. S. Rowland, Hydrocarbon and halocarbon measurements as photochemical and dynamical indicators of atmospheric hydroxyl, atomic chlorine, and vertical mixing obtained during Lagrangian flights, *J. Geophys. Res. Atmos.*, 1996, **101**, 4331–4340.

87 M. R. McGillen, W. P. L. Carter, A. Mellouki, J. J. Orlando, B. Picquet-Varrault and T. J. Wallington, Database for the kinetics of the gas-phase atmospheric reactions of organic compounds, *Earth Syst. Sci. Data*, 2020, **12**, 1203–1216.

88 M. R. McGillen, W. P. L. Carter, A. Mellouki, J. J. Orlando, B. Picquet-Varrault and T. J. Wallington, *Database for the Kinetics of the Gas-Phase Atmospheric Reactions of Organic Compounds*, 2023, DOI: 10.25326/abq8-f406.

89 S. Vijayakumar and B. Rajakumar, Theoretical investigations on the kinetics of Cl atom initiated reactions of series of 1-alkenes, *Environ. Sci. Pollut. Res.*, 2017, **25**, 4387–4405.

90 J. Zhu, S. Wang, N. T. Tsona, X. Jiang, Y. Wang, M. Ge and L. Du, Gas-Phase Reaction of Methyl n-Propyl Ether with OH, NO₃, and Cl: Kinetics and Mechanism, *J. Phys. Chem. A*, 2017, **121**, 6800–6809.

91 M. B. Blanco, I. Barnes and M. A. Teruel, FTIR gas-phase kinetic study of the reactions of Cl atoms with (CH₃)₂CCHC(O)H and CH₃CHCHC(O)OCH₃, *Chem. Phys. Lett.*, 2010, **488**, 135–139.

92 A. Grira, C. Amarandei, M. N. Romanias, G. El Dib, A. Canosa, C. Arsene, I. G. Bejan, R. I. Olariu, P. Coddeville and A. Tomas, Kinetic Measurements of Cl Atom Reactions with C₅–C₈ Unsaturated Alcohols, *Atmosphere*, 2020, **11**, 256.

93 S. M. Aschmann and R. Atkinson, Rate Constants for the Gas-Phase Reactions of Alkanes with Cl Atoms at 296 ± 2 K, *Int. J. Chem. Kinet.*, 1995, **27**, 613–622.

94 B. Shi, W. Wang, L. Zhou, Z. Sun, C. Fan, Y. Chen, W. Zhang, Y. Qiao, Y. Qiao and M. Ge, Atmospheric oxidation of C₁₀₋₁₄ n-alkanes initiated by Cl atoms: Kinetics and mechanism, *Atmos. Environ.*, 2020, **222**, 117166.

95 Y. Chen, W. Wang, J. Li, L. Zhou, B. Shi, C. Fan, K. Wang, H. Zhang, H. Li and M. Ge, Kinetic and mechanism of the reaction between Cl and several mono-methyl branched alkanes, *J. Environ. Sci.*, 2024, **135**, 474–482.

96 J. Albaladejo, A. Notario, C. A. Cuevas, E. Jiménez, B. Cabañas and E. Martínez, Gas-phase chemistry of atmospheric Cl atoms:: a PLP-RF kinetic study with a series of ketones, *Atmos. Environ.*, 2003, **37**, 455–463.

97 S. Wang, L. Du, N. T. Tsona and W. Wang, Gas-phase kinetic and mechanism study of the reactions of O₃, OH, Cl and NO₃ with unsaturated acetates, *Environ. Chem.*, 2018, **15**, 411–423.

98 B. Cabanas, F. Villanueva, P. Martin, M. Baeza, S. Salgado and E. Jimenez, Study of reaction processes of furan and some furan derivatives initiated by Cl atoms, *Atmos. Environ.*, 2005, **39**, 1935–1944.

99 E. S. C. Kwok and R. Atkinson, Estimation of hydroxyl radical reaction rate constants for gas-phase organic compounds using a structure-reactivity relationship: An update, *Atmos. Environ.*, 1995, **29**, 1685–1695.

100 R. A. Taccone, A. Moreno, I. Colmenar, S. Salgado, M. P. Martín and B. Cabañas, Kinetic study of the OH, NO₃ radicals and Cl atom initiated atmospheric photo-oxidation of iso-propenyl methyl ether, *Atmos. Environ.*, 2016, **127**, 80–89.

101 A. Guenther, C. N. Hewitt, D. Erickson, R. Fall, C. Geron, T. Graedel, P. Harley, L. Klinger, M. Lerdau, W. A. McKay, T. Pierce, B. Scholes, R. Steinbrecher, R. Tallamraju, J. Taylor and P. Zimmerman, A global model of natural volatile organic compound emissions, *J. Geophys. Res. Atmos.*, 1995, **100**, 8873–8892.

102 R. Atkinson and J. Arey, Atmospheric degradation of volatile organic compounds, *Chem. Rev.*, 2003, **103**, 4605–4638.

103 P. J. Ziemann and R. Atkinson, Kinetics, products, and mechanisms of secondary organic aerosol formation, *Chem. Soc. Rev.*, 2012, **41**, 6582–6605.

104 C. J. Young, R. A. Washenfelder, P. M. Edwards, D. D. Parrish, J. B. Gilman, W. C. Kuster, L. H. Mielke, H. D. Osthoff, C. Tsai, O. Pikelnaya, J. Stutz, P. R. Veres, J. M. Roberts, S. Griffith, S. Dusanter, P. S. Stevens, J. Flynn, N. Grossberg, B. Lefer, J. S. Holloway, J. Peischl, T. B. Ryerson, E. L. Atlas, D. R. Blake and S. S. Brown, Chlorine as a primary radical: evaluation of methods to understand its role in initiation of oxidative cycles, *Atmos. Chem. Phys.*, 2014, **14**, 3427–3440.

105 Y. Wang, M. Riva, H. Xie, L. Heikkinen, S. Schallhart, Q. Zha, C. Yan, X.-C. He, O. Peräkylä and M. Ehn, Formation of highly oxygenated organic molecules from chlorine-atom-initiated oxidation of alpha-pinene, *Atmos. Chem. Phys.*, 2020, **20**, 5145–5155.

© 2026 The Author(s). Published by the Royal Society of Chemistry

Environ. Sci.: Atmos., 2026, **6**, 7–26 | 23

106 M. M. Maricq, J. J. Szente, E. W. Kaiser and J. C. Shi, Reaction of Chlorine Atoms with Methylperoxy and Ethylperoxy Radicals, *J. Phys. Chem.*, 1994, **98**, 2083–2089.

107 A. M. Avery, M. W. Alton, M. R. Canagaratna, J. E. Krechmer, D. T. Sueper, N. Bhattacharyya, L. Hildebrandt Ruiz, W. H. Brune and A. T. Lambe, Comparison of the Yield and Chemical Composition of Secondary Organic Aerosol Generated from the OH and Cl Oxidation of Decamethylcyclopentasiloxane, *ACS Earth Space Chem.*, 2023, **7**, 218–229.

108 Y. B. Lim and P. J. Ziemann, Kinetics of the heterogeneous conversion of 1,4-hydroxycarbonyls to cyclic hemiacetals and dihydrofurans on organic aerosol particles, *Phys. Chem. Chem. Phys.*, 2009, **11**, 8029–8039.

109 C. E. Jordan, P. J. Ziemann, R. J. Griffin, Y. B. Lim, R. Atkinson and J. Arey, Modeling SOA formation from OH reactions with C_8-C_{17} n-alkanes, *Atmos. Environ.*, 2008, **42**, 8015–8026.

110 R. Atkinson, J. Arey and S. M. Aschmann, Atmospheric chemistry of alkanes: Review and recent developments, *Atmos. Environ.*, 2008, **42**, 5859–5871.

111 D. S. Wang and L. Hildebrandt Ruiz, Chlorine-initiated oxidation of n-alkanes under high-NOx conditions: insights into secondary organic aerosol composition and volatility using a FIGAERO–CIMS, *Atmos. Chem. Phys.*, 2018, **18**, 15535–15553.

112 P. O. Wennberg, K. H. Bates, J. D. Crounse, L. G. Dodson, R. C. McVay, L. A. Mertens, T. B. Nguyen, E. Praske, R. H. Schwantes, M. D. Smarte, J. M. St Clair, A. P. Teng, X. Zhang and J. H. Seinfeld, Gas-Phase Reactions of Isoprene and Its Major Oxidation Products, *Chem. Rev.*, 2018, **118**, 3337–3390.

113 Y. Bedjanian, G. Laverdet and G. Le Bras, Low-pressure study of the reaction of Cl atoms with isoprene, *J. Phys. Chem. A*, 1998, **102**, 953–959.

114 I. Suh and R. Y. Zhang, Kinetic studies of isoprene reactions initiated by chlorine atom, *J. Phys. Chem. A*, 2000, **104**, 6590–6596.

115 J.-H. Xing, K. Takahashi, M. D. Hurley and T. J. Wallington, Kinetics of the reaction of chlorine atoms with isoprene (2-methyl 1,3-butadiene, $CH_2=C(CH_3)CH=CH_2$ at 297 ± 2 K, *Chem. Phys. Lett.*, 2009, **472**, 39–43.

116 D. S. Wang and L. H. Ruiz, Secondary organic aerosol from chlorine-initiated oxidation of isoprene, *Atmos. Chem. Phys.*, 2017, **17**, 13491–13508.

117 M. Walavalkar, A. Sharma, H. D. Alwe, K. K. Pushpa, S. Dhanya, P. D. Naik and P. N. Bajaj, Cl atom initiated oxidation of 1-alkenes under atmospheric conditions, *Atmos. Environ.*, 2013, **67**, 93–100.

118 R. S. Karlsson, J. J. Szente, J. C. Ball and M. M. J. T. Maricq, Homogeneous aerosol formation by the chlorine atom initiated oxidation of toluene, *J. Phys. Chem. A*, 2001, **105**, 82–96.

119 G. Fantechi, N. R. Jensen, O. Saastad, J. Hjorth and J. Peeters, Reactions of Cl atoms with selected VOCs: Kinetics, products and mechanisms, *J. Atmos. Chem.*, 1998, **31**, 247–267.

120 C. Fan, W. Wang, B. Shi, Z. Sun and M. Ge, Experimental and Theoretical Study of Unsaturated Alcohol Reaction with Cl Atoms: Kinetics, Products, and Mechanisms, *ACS Earth Space Chem.*, 2024, **8**, 2621–2632.

121 R. G. Gibilisco, I. Bejan, I. Barnes, P. Wiesen and M. A. Teruel, Rate coefficients at 298 K and 1 atm for the tropospheric degradation of a series of C_6, C_7 and C_8 biogenic unsaturated alcohols initiated by Cl atoms, *Atmos. Environ.*, 2014, **94**, 564–572.

122 Y. Gai, M. Ge and W. Wang, Kinetics of the gas-phase reactions of some unsaturated alcohols with Cl atoms and O_3, *Atmos. Environ.*, 2011, **45**, 53–59.

123 X. Lin, R. Hu, Z. Ma, H. Yue, Z. Wen, C. Zhang, C. Fittschen, W. Zhang and X. Tang, Cl-Initiated oxidation of methacrolein under NOx-free conditions studied by VUV photoionization mass spectrometry, *Phys. Chem. Chem. Phys.*, 2022, **24**, 17471–17478.

124 K. Shashikala and D. Janardanan, Degradation mechanism of trans-2-hexenal in the atmosphere, *Chem. Phys. Lett.*, 2020, **759**, 138039.

125 A. Grira, M. Antiñolo, A. Canosa, A. Tomas, G. El Dib and E. Jiménez, Kinetic and Products Study of the Atmospheric Degradation of trans-2-Hexenal with Cl Atoms, *J. Phys. Chem. A*, 2022, **126**, 6973–6983.

126 L. K. Xue, S. M. Saunders, T. Wang, R. Gao, X. F. Wang, Q. Z. Zhang and W. X. Wang, Development of a chlorine chemistry module for the Master Chemical Mechanism, *Geosci. Model Dev.*, 2015, **8**, 3151–3162.

127 J. Tröstl, W. K. Chuang, H. Gordon, M. Heinritzi, C. Yan, U. Molteni, L. Ahlm, C. Frege, F. Bianchi, R. Wagner, M. Simon, K. Lehtipalo, C. Williamson, J. S. Craven, J. Duplissy, A. Adamov, J. Almeida, A.-K. Bernhammer, M. Breitenlechner, S. Brilke, A. Dias, S. Ehrhart, R. C. Flagan, A. Franchin, C. Fuchs, R. Guida, M. Gysel, A. Hansel, C. R. Hoyle, T. Jokinen, H. Junninen, J. Kangasluoma, H. Keskinen, J. Kim, M. Krapf, A. Kürten, A. Laaksonen, M. Lawler, M. Leiminger, S. Mathot, O. Möhler, T. Nieminen, A. Onnela, T. Petäjä, F. M. Piel, P. Miettinen, M. P. Rissanen, L. Rondo, N. Sarnela, S. Schobesberger, K. Sengupta, M. Sipilä, J. N. Smith, G. Steiner, A. Tomè, A. Virtanen, A. C. Wagner, E. Weingartner, D. Wimmer, P. M. Winkler, P. Ye, K. S. Carslaw, J. Curtius, J. Dommen, J. Kirkby, M. Kulmala, I. Riipinen, D. R. Worsnop, N. M. Donahue and U. Baltensperger, The role of low-volatility organic compounds in initial particle growth in the atmosphere, *Nature*, 2016, **533**, 527–531.

128 Z. Ling, L. Wu, Y. Wang, M. Shao, X. Wang and W. Huang, Roles of semivolatile and intermediate-volatility organic compounds in secondary organic aerosol formation and its implication: A review, *J. Environ. Sci.*, 2022, **114**, 259–285.

129 C. L. Loza, J. S. Craven, L. D. Yee, M. M. Coggon, R. H. Schwantes, M. Shiraiwa, X. Zhang, K. A. Schilling, N. L. Ng, M. R. Canagaratna, P. J. Ziemann, R. C. Flagan and J. H. Seinfeld, Secondary organic aerosol yields of 12-carbon alkanes, *Atmos. Chem. Phys.*, 2014, **14**, 1423–1439.

130 L. G. Jahn, D. S. Wang, S. V. Dhulipala and L. H. Ruiz, Gas-Phase Chlorine Radical Oxidation of Alkanes: Effects of Structural Branching, NOx, and Relative Humidity Observed during Environmental Chamber Experiments, *J. Phys. Chem. A*, 2021, **125**, 7303–7317.

131 J. F. Hunter, A. J. Carrasquillo, K. E. Daumit and J. H. Kroll, Secondary Organic Aerosol Formation from Acyclic, Monocyclic, and Polycyclic Alkanes, *Environ. Sci. Technol.*, 2014, **48**, 10227–10234.

132 Y. B. Lim and P. J. Ziemann, Effects of Molecular Structure on Aerosol Yields from OH Radical-Initiated Reactions of Linear, Branched, and Cyclic Alkanes in the Presence of NOx, *Environ. Sci. Technol.*, 2009, **43**, 2328–2334.

133 J. Liu, E. L. D'Ambro, B. H. Lee, F. D. Lopez-Hilfiker, R. A. Zaveri, J. C. Rivera-Rios, F. N. Keutsch, S. Iyer, T. Kurten, Z. Zhang, A. Gold, J. D. Surratt, J. E. Shilling and J. A. Thornton, Efficient Isoprene Secondary Organic Aerosol Formation from a Non-IEPOX Pathway, *Environ. Sci. Technol.*, 2016, **50**, 9872–9880.

134 X. Cai and R. J. Griffin, Secondary aerosol formation from the oxidation of biogenic hydrocarbons by chlorine atoms, *J. Geophys. Res. Atmos.*, 2006, **111**, D14206.

135 S. V. Dhulipala, S. Bhandari and L. Hildebrandt Ruiz, Formation of oxidized organic compounds from Cl-initiated oxidation of toluene, *Atmos. Environ.*, 2019, **199**, 265–273.

136 N. L. Ng, J. H. Kroll, A. W. H. Chan, P. S. Chhabra, R. C. Flagan and J. H. Seinfeld, Secondary organic aerosol formation from m-xylene, toluene, and benzene, *Atmos. Chem. Phys.*, 2007, **7**, 3909–3922.

137 K. M. Shakya and R. J. Griffin, Secondary Organic Aerosol from Photooxidation of Polycyclic Aromatic Hydrocarbons, *Environ. Sci. Technol.*, 2010, **44**, 8134–8139.

138 F. Pan, J. Ma, Q. Yan, G. Zhao, B. Jia, L. Xu and P. Cheng, Formation of secondary organic aerosols from Cl-initiated oxidation of anisole: Rapid release of ultrafine particles and organic chlorides, *Atmos. Environ.*, 2024, **329**, 120544.

139 C. Li, M. V. Misovich, M. Pardo, Z. Fang, A. Laskin, J. Chen and Y. Rudich, Secondary organic aerosol formation from atmospheric reactions of anisole and associated health effects, *Chemosphere*, 2022, **308**, 136421.

140 A. T. Lambe, A. M. Avery, N. Bhattacharyya, D. S. Wang, M. Modi, C. G. Masoud, L. H. Ruiz and W. H. Brune, Comparison of secondary organic aerosol generated from the oxidation of laboratory precursors by hydroxyl radicals, chlorine atoms, and bromine atoms in an oxidation flow reactor, *Environ. Sci.: Atmos.*, 2022, **2**, 687–701.

141 L. Li, P. Tang, S. Nakao and D. R. Cocker Iii, Impact of molecular structure on secondary organic aerosol formation from aromatic hydrocarbon photooxidation under low-NOx conditions, *Atmos. Chem. Phys.*, 2016, **16**, 10793–10808.

142 C. Bloss, V. Wagner, M. E. Jenkin, R. Volkamer, W. J. Bloss, J. D. Lee, D. E. Heard, K. Wirtz, M. Martin-Reviejo, G. Rea, J. C. Wenger and M. J. Pilling, Development of a detailed chemical mechanism (MCMv3.1) for the atmospheric oxidation of aromatic hydrocarbons, *Atmos. Chem. Phys.*, 2005, **5**, 641–664.

143 C. R. Stephens, P. B. Shepson, A. Steffen, J. W. Bottenheim, J. Liao, L. G. Huey, E. Apel, A. Weinheimer, S. R. Hall, C. Cantrell, B. C. Sive, D. J. Knapp, D. D. Montzka and R. S. Hornbrook, The relative importance of chlorine and bromine radicals in the oxidation of atmospheric mercury at Barrow, Alaska, *J. Geophys. Res. Atmos.*, 2012, **117**, D14.

144 A. T. Lambe, P. S. Chhabra, T. B. Onasch, W. H. Brune, J. F. Hunter, J. H. Kroll, M. J. Cummings, J. F. Brogan, Y. Parmar, D. R. Worsnop, C. E. Kolb and P. Davidovits, Effect of oxidant concentration, exposure time, and seed particles on secondary organic aerosol chemical composition and yield, *Atmos. Chem. Phys.*, 2015, **15**, 3063–3075.

145 E. Kang, D. W. Toohey and W. H. Brune, Dependence of SOA oxidation on organic aerosol mass concentration and OH exposure: experimental PAM chamber studies, *Atmos. Chem. Phys.*, 2011, **11**, 1837–1852.

146 J. H. Kroll, J. D. Smith, D. L. Che, S. H. Kessler, D. R. Worsnop and K. R. Wilson, Measurement of fragmentation and functionalization pathways in the heterogeneous oxidation of oxidized organic aerosol, *Phys. Chem. Chem. Phys.*, 2009, **11**, 8005–8014.

147 X. Ma, K. Li, S. Zhang, Z. Yang, L. Xu, N. Tsona Tchinda and L. Du, Oxidation Flow Reactor and Its Application in Secondary Organic Aerosol Formation in Laboratory Studies, *ACS ES&T Air*, 2025, **2**, 1394–1410.

148 S. Liu, Y. Wang, S. Zhang, Y. Chen, C. Wu, G. Zhang and G. Wang, The synergistic effect of NOx and SO$_2$ on the formation and light absorption of secondary organic aerosols from o-xylene photooxidation, *Atmos. Res.*, 2024, **304**, 107387.

149 Z. Wang, F. Couvidat and K. Sartelet, Response of biogenic secondary organic aerosol formation to anthropogenic NOx emission mitigation, *Sci. Total Environ.*, 2024, **927**, 172142.

150 C. G. Masoud and L. H. Ruiz, Chlorine-Initiated Oxidation of α-Pinene: Formation of Secondary Organic Aerosol and Highly Oxygenated Organic Molecules, *ACS Earth Space Chem.*, 2021, **5**, 2307–2319.

151 J. J. Orlando, G. S. Tyndall and T. J. Wallington, The atmospheric chemistry of alkoxy radicals, *Chem. Rev.*, 2003, **103**, 4657–4690.

152 Z. Wang, M. Ehn, M. P. Rissanen, O. Garmash, L. Quéléver, L. Xing, M. Monge-Palacios, P. Rantala, N. M. Donahue, T. Berndt and S. M. Sarathy, Efficient alkane oxidation under combustion engine and atmospheric conditions, *Commun. Chem.*, 2021, **4**, 18.

153 X. Peng, T.-T. Xie, M.-X. Tang, Y. Cheng, Y. Peng, F.-H. Wei, L.-M. Cao, K. Yu, K. Du, L.-Y. He and X.-F. Huang, Critical Role of Secondary Organic Aerosol in Urban Atmospheric Visibility Improvement Identified by Machine Learning, *Environ. Sci. Technol. Lett.*, 2023, **10**, 976–982.

154 K. Zhang, L. Li, L. Huang, Y. Wang, J. Huo, Y. Duan, Y. Wang and Q. Fu, The impact of volatile organic compounds on ozone formation in the suburban area of Shanghai, *Atmos. Environ.*, 2020, **232**, 117511.

© 2026 The Author(s). Published by the Royal Society of Chemistry

Environ. Sci.: Atmos., 2026, **6**, 7–26 | 25

155 J. K. Bean and L. Hildebrandt Ruiz, Gas-particle partitioning and hydrolysis of organic nitrates formed from the oxidation of α-pinene in environmental chamber experiments, *Atmos. Chem. Phys.*, 2016, **16**, 2175–2184.

156 J. D. Rindelaub, C. H. Borca, M. A. Hostetler, J. H. Slade, M. A. Lipton, L. V. Slipchenko and P. B. Shepson, The acid-catalyzed hydrolysis of an α-pinene-derived organic nitrate: kinetics, products, reaction mechanisms, and atmospheric impact, *Atmos. Chem. Phys.*, 2016, **16**, 15425–15432.

157 M. L. Hinks, J. Montoya-Aguilera, L. Ellison, P. Lin, A. Laskin, J. Laskin, M. Shiraiwa, D. Dabdub and S. A. Nizkorodov, Effect of relative humidity on the composition of secondary organic aerosol from the oxidation of toluene, *Atmos. Chem. Phys.*, 2018, **18**, 1643–1652.

158 M. S. Jang, N. M. Czoschke, S. Lee and R. M. Kamens, Heterogeneous atmospheric aerosol production by acid-catalyzed particle-phase reactions, *Science*, 2002, **298**, 814–817.

159 Z. Luo, H. Zang, Z. Li, C. Li and Y. Zhao, Species-specific effect of particle viscosity and particle-phase reactions on the formation of secondary organic aerosol, *Sci. Total Environ.*, 2024, **950**, 175207.

160 L. Renbaum-Wolff, J. W. Grayson, A. P. Bateman, M. Kuwata, M. Sellier, B. J. Murray, J. E. Shilling, S. T. Martin and A. K. Bertram, Viscosity of α-pinene secondary organic material and implications for particle growth and reactivity, *Proc. Natl. Acad. Sci. U. S. A.*, 2013, **110**, 8014–8019.

161 G. Chen, Z. Chen, Y. Zhang, X. Fan, L. Xu, Z. Lin, X. Ji and J. Chen, Enhanced oxidation capacity driven by pollution-induced chlorine chemistry in the coastal atmosphere, *npj Clim. Atmos. Sci.*, 2025, **8**, 248.

162 J. D. Haskins, B. H. Lee, F. D. Lopez-Hilifiker, Q. Peng, L. Jaeglé, J. M. Reeves, J. C. Schroder, P. Campuzano-Jost, D. Fibiger, E. E. McDuffie, J. L. Jiménez, S. S. Brown and J. A. Thornton, Observational Constraints on the Formation of Cl_2 From the Reactive Uptake of $ClNO_2$ on Aerosols in the Polluted Marine Boundary Layer, *J. Geophys. Res. Atmos.*, 2019, **124**, 8851–8869.

163 G. McFiggans, T. F. Mentel, J. Wildt, I. Pullinen, S. Kang, E. Kleist, S. Schmitt, M. Springer, R. Tillmann, C. Wu, D. F. Zhao, M. Hallquist, C. Faxon, M. Le Breton, Å. Hallquist, D. Simpson, R. Bergström, M. E. Jenkin, M. Ehn, J. A. Thornton, M. R. Alfarra, T. J. Bannan, C. J. Percival, M. Priestley, D. Topping and A. Kiendler-Scharr, Secondary organic aerosol reduced by mixture of atmospheric vapours, *Nature*, 2019, **565**, 587–593.

164 J. Li, H. Li, K. Li, Y. Chen, H. Zhang, X. Zhang, Z. Wu, Y. Liu, X. Wang, W. Wang and M. Ge, Enhanced secondary organic aerosol formation from the photo-oxidation of mixed anthropogenic volatile organic compounds, *Atmos. Chem. Phys.*, 2021, **21**, 7773–7789.

165 S. J. Liu, T. Galeazzo, R. Valorso, M. Shiraiwa, C. L. Faiola and S. A. Nizkorodov, Secondary Organic Aerosol from OH-Initiated Oxidation of Mixtures of D-Limonene and β-Myrcene, *Environ. Sci. Technol.*, 2024, **58**, 13391–13401.